R-03-23

On the role of mesh discretisation and salinity for the occurrence of local flow cells

Results from a regional-scale groundwater flow model of Östra Götaland

Sven Follin, SF GeoLogic AB
Urban Svensson, Computer-aided Fluid Engineering AB

June 2003

Svensk Kärnbränslehantering AB
Swedish Nuclear Fuel
and Waste Management Co
Box 5864
SE-102 40 Stockholm Sweden
Tel 08-459 84 00
+46 8 459 84 00
Fax 08-661 57 19
+46 8 661 57 19

ISSN 1402-3091
SKB Rapport R-03-23

On the role of mesh discretisation and salinity for the occurrence of local flow cells

Results from a regional-scale groundwater flow model of Östra Götaland

Sven Follin, SF GeoLogic AB
Urban Svensson, Computer-aided Fluid Engineering AB

June 2003

Abstract

Results from a regional-scale groundwater flow model of Östra Götaland suggest that local-scale variations in the topography together with groundwater salinity have a large impact on the groundwater flow pattern in the Fennoscandian shield. This in turn, rejects the reasoning that regional-scale topography is a major mechanism for groundwater flow from the inland of Östra Götaland. On the contrary, most recharge and discharge areas seem to be fairly close together regardless of the distance to the coast, which implies that it is the local-scale topography and the hydrogeological properties at each site that will by and large determine the transport times.

The model was used to run numerical simulations of variable-density groundwater flow in a 270 km long, 210 km wide and approximately 10 km deep three-dimensional domain. The simulations were run for two different mesh discretisations, thus honouring different resolutions of the local-scale variations in the topography. The model with the coarser mesh discretisation was used to mimic the flow model by /Voss and Provost, 2001/, who claim that inland nuclear waste repositories may provide a higher hydrogeological safety margin than coastal nuclear waste repositories because of the regional-scale groundwater flow pattern. The model with the finer mesh discretisation was used to scrutinise the results of the former. Simulation results demonstrate the great impact of the chosen mesh discretisation on the model results and that regional-scale topography is not a major mechanism for groundwater flow at repository depth in comparison with local-scale variations in the topography.

Simulations with variable fluid density differ from those with constant fluid density. The simulation results confirm that groundwater salinity limits the penetration depth of the freshwater flowpaths, which in effect boosts the role of the local-scale variations in the topography with regards to the role of regional flow.

Sammanfattning

Resultaten från en regional grundvattenmodell över Östra Götaland indikerar att de lokala variationerna i topografin tillsammans med förekomsten av salint grundvatten har stor påverkan på flödesmönstret. Studien antyder att regional topografi inte är en huvudmekanism för grundvattenströmning från inlandslägen i Östra Götaland. Tvärtom förefaller merparten av alla inströmningsområden och utströmningsområden ligga förhållandevis nära varandra oavsett avståndet till kusten, vilket indikerar att det är den lokala topografin och de platsspecifika hydrogeologiska egenskaperna som i huvudsak avgör beräknade transporttider.

Beräkningsmodellen användes för att simulera variabel densitetsströmning i en 270 km lång, 210 km bred och approximativt 10 km djup tredimensionell modelldomän. Simuleringar gjordes med två olika modellnät, vilket innebär olika hänsynstagande till de lokala variationerna i topografin. Modellen med den grövre diskretiseringen användes för att efterlikna en flödesmodell gjord av /Voss och Provost, 2001/, vilka menar att avfallsförvar i inlandet erbjuder större säkerhetsmarginal ur hydrogeologisk synvinkel än kustnära avfallsförvar pga regional grundvattenströmning. Modellen med den finare diskretiseringen användes för att analysera resultaten från modellen med den grövre diskretiseringen. Simuleringar med de två modellnäten visar att den valda diskretiseringen i hög grad påverkar beräkningsresultaten och att regional topografi är av mindre betydelse för grundvattenströmningen på aktuell förvarsnivå jämfört med lokala variationer i topografin.

Simuleringar med variabel fluiddensitet skiljer sig från simuleringar med konstant fluiddensitet. Resultaten bekräftar att grundvattnets salinitet begränsar de nedåtgående flödesvägarnas djupgående, vilket i sin tur förstärker betydelsen av de lokala variationerna i topografin.

Contents

1 Introduction

1.1 Background

As a result of their assessment of the documentation prior to the selection of candidate sites for further investigations /SKB, 2000/, the Swedish authorities SKI and SSI requested that SKB must provide a better background material for the evaluation of recharge and discharge areas and of the depth to saline groundwater as site selection factors. Subsequent discussions have been concerned with issues dealing with the physical siting of a nuclear waste repository with regards to recharge and discharge areas and if it matters if the repository gets an inland or coastal location.

1.2 Objectives

The overall objective of the study is to contribute to the understanding and evaluation of processes affecting the distribution of recharge and discharge areas on a regional scale in the Fennoscandian shield. For the most part the study focuses on the role of two specific issues – local topographic variations and the depth to saline groundwater.

Appendix A presents simulation results from a comparison between the computer code used in the present study and the computer code used in a parallel study conducted by /Holmén et al, 2003/. Besides topography, /Holmén et al, 2003/ studied the role of geological features such as fracture zones, clay layers, etc. However, /Holmén et al, 2003/ studied a different model domain than the one treated in the present study. The objective with Appendix A is to cross-validate the two computer codes and thereby indirectly corroborate the numerical results of the two studies.

Appendix B presents simulation results concerning the recharge and discharge pattern within the Simpevarp Candidate Area using a fine mesh discretisation. It is noted here that the work presented in Appendix B is an extension of the original scope of the present study, which from the onset was not intended to deal with the recharge and discharge pattern of specific sites.

1.3 Scope

The study is based on a regional-scale groundwater flow model of southeast Sweden, commonly referred to as Östra Götaland. The model was used to run numerical simulations of variable-density groundwater flow in a 270 km long, 210 km wide and approximately 10 km deep three-dimensional domain, see Figure 1-1.

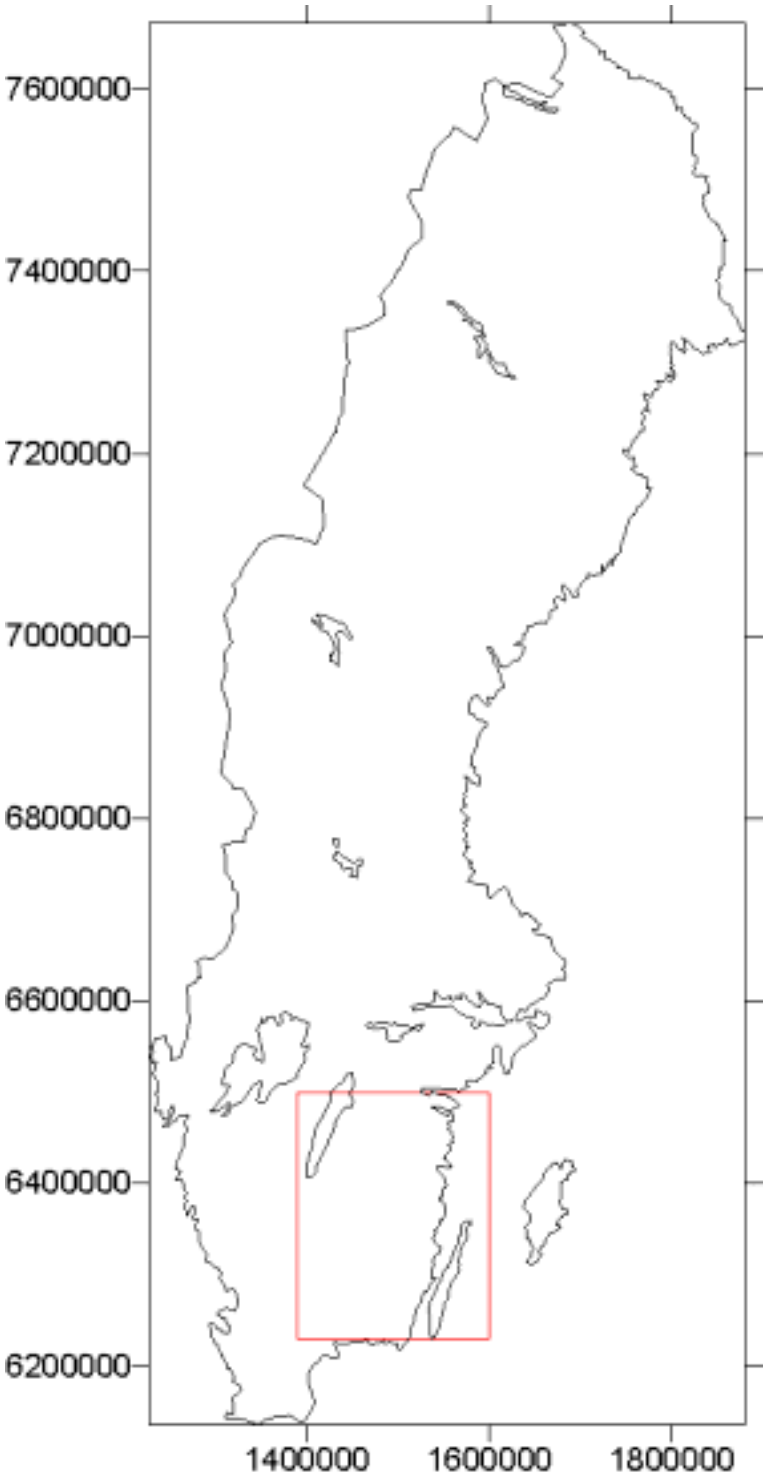

Figure 1-1. *Contour of Sweden and the location of the model area, Östra Götaland.*

The simulations were run for two different mesh discretisations, thus honouring the local-scale variations in the topography differently, see Figure 1-2 and Figure 1-3. The model with the coarser mesh discretisation was used to mimic the flow model by /Voss and Provost, 2001/. The model with the finer mesh discretisation was used to scrutinise the results of the former. In addition, the role of variable-density groundwater flow was studied by repeating some of the simulations without salinity.

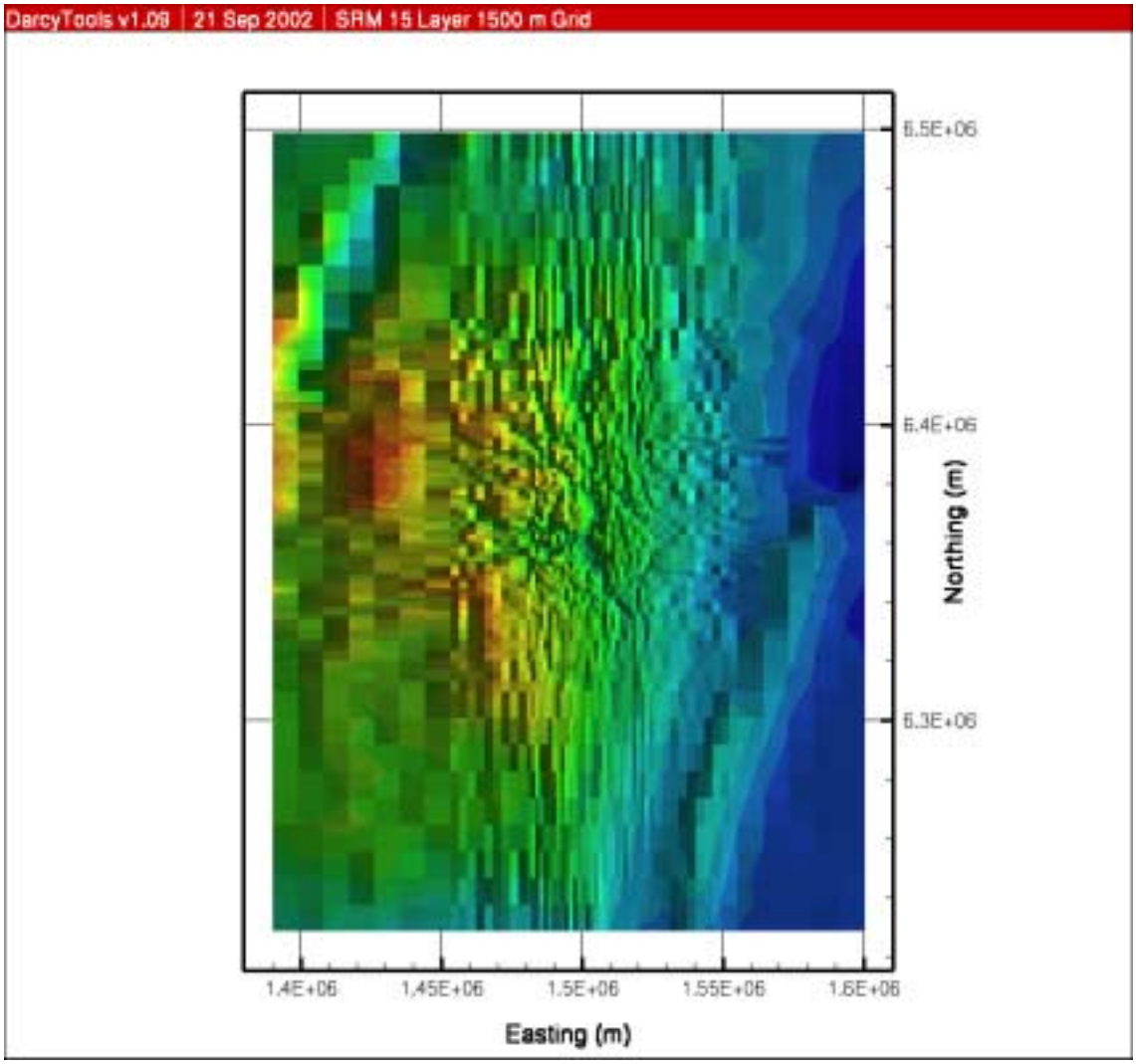

Figure 1-2. *Visualisation of the topography and bathymetry within the model domain using a coarse mesh discretisation. The horizontal resolution is 1 500 m in the centre and 9 000 m in the corners. This setting mimics the mesh discretisation used by /Voss and Provost, 2001/.*

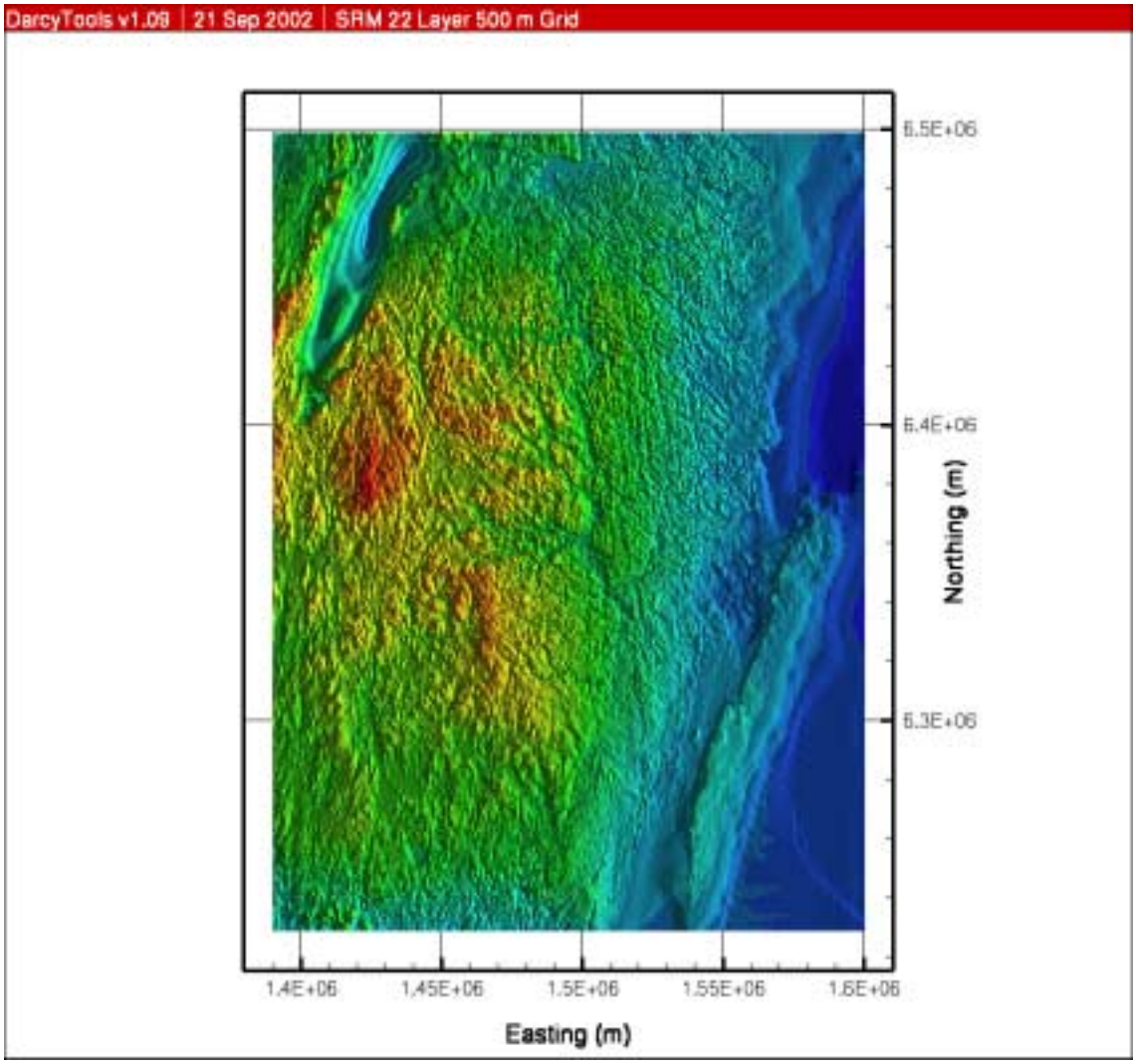

Figure 1-3. *Visualisation of the topography and bathymetry within the model domain using a fine mesh discretisation. The horizontal resolution is 500 m throughout the model domain.*

1.4 Outline of report

Chapter 2 presents some of the previous work carried out on the matters of interest. It also presents the topography and regional runoff of southeast Sweden. The groundwater flow model setup is presented in Chapter 3. The simulation results are shown in Chapter 4. The discussion and conclusions are found in Chapter 5.

2 Recharge and discharge areas

2.1 Previous work

The dependence of the groundwater flow pattern on the topography was demonstrated already back in the 1960's by /Tóth, 1963/, which constitutes a classic reference in the hydrogeological literature. Among the large body of previous work dealing with groundwater recharge and discharge, the contributions of /Freeze and Witherspoon, 1967/ and /Zijl, 1999/ should also be noted. Some Swedish studies on the subject are, among others, /Gustafsson, 1970/, /Voss and Andersson, 1993/ and /Rehbinder et al, 1997/.

/Tóth, 1963/ showed that the relationship between the regional and local topographic gradients governs the spatial distribution and depth of the groundwater flow cells. /Zijl, 1999/ elaborated the analysis and demonstrated quantitatively how the depth of the flow cells can be expressed as a function of the anisotropy of the hydraulic conductivity and the wavelength of the spatial variability in the topography.

Figure 2-1 shows three images from /Freeze and Witherspoon, 1967/, which demonstrate the concept of flow cells. The three model cross-sections of groundwater flow differ with regards to the local variations in the topography and, hence, the looks of the groundwater table. The cross-sections are based on numerical simulations using simplified geological conditions, which are assumed to be two-dimensional, isotropic and homogeneous. Compared to cross-section A, cross-section B demonstrates that a topographic high, small or large, creates a local recharge area. Likewise, a topographic low creates a local discharge area. A spatially varying topography as in cross-section C creates a number of local and/or intermediary flow cells. It is noted that the local variations in the topography govern the small-scale surface runoff and that some of the recharge, although to a limited extent, may surpass the local drainage basins. That is, regional groundwater divides do not necessarily always coincide with the local ones.

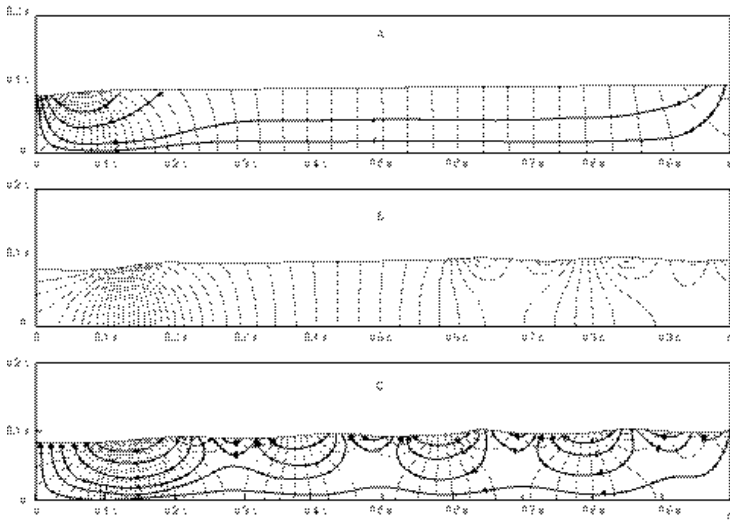

Figure 2-1. *Visualisation of the impact of the shape of the groundwater table on the regional groundwater flow pattern /from Freeze and Witherspoon, 1967/.*

2.2 On the physical siting of a nuclear waste repository

/Tóth and Sheng, 1996/ advocated that the flow cell theory implies that nuclear waste repositories should be sited in regional recharge areas rather than discharge areas. /Voss and Provost, 2001/ used a three-dimensional variable-density flow model in combination with the topography of a specific location, Östra Götaland, to demonstrate the reasoning. Given the conclusions by Voss and Provost, a coastal repository appears as less favourable compared to a repository with an inland location.

The effects of combining topographic gradients with density driven flow using generic data for Östra Götaland was previously studied by /Voss and Andersson, 1993/ using a two-dimensional variable-density flow model. Voss and Andersson concluded that the groundwater flow in the upper parts of the subsurface is not significantly affected by the salinity due to the ongoing shoreline displacement. Voss and Andersson also concluded that local topographic gradients and fracture zones result in quite complex flow patterns.

2.3 Topography and regional runoff of Östra Götaland

Figure 2-2 shows two images of the model area from Voss and Provost. The image to the left illustrates the topography of Östra Götaland together with the four exploratory sites treated (purple polygons). Two of the four sites have a coastal location, Simpevarp and Oskarshamn Södra, whereas the other two have an inland location, Hultsfred Östra and the Comparison Site. The Comparison Site is located at the crest of the southern Swedish highlands, c 350 m a s l. The mesh used is shown to the right. The horizontal resolution varies between 1 500–9 000 m.

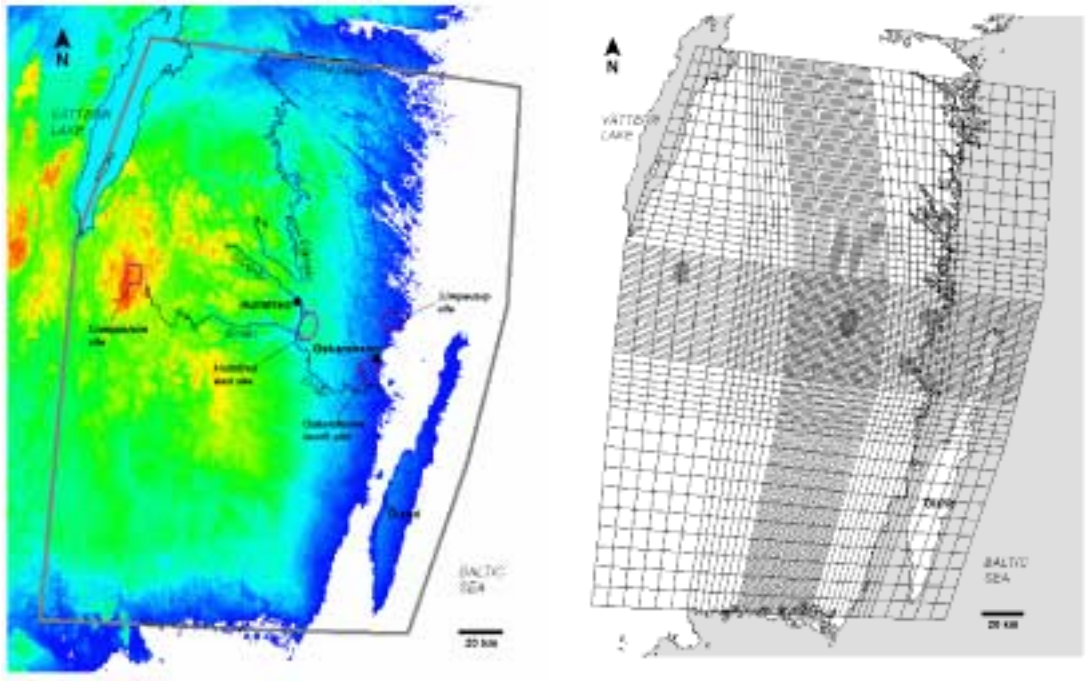

Figure 2-2. *Two images from /Voss and Provost, 2001/. Left: The topography of Östra Götaland together with the four exploratory sites treated. Right: Model mesh. The horizontal mesh discretisation varies between 1 500–9 000 m.*

The left image of Figure 2-3 shows the mesh discretisation used in the present study to mimic the mesh discretisation shown in Figure 2-2. The left image also shows the locations of the four exploratory sites. The topographic variations along the red line running from west to east are scrutinised in Figure 2-4 and Figure 2-5.

The geometrical difference between the two meshes as far as the shapes of the finite elements and the finite difference cells are concerned is insignificant for the problem of interest. The major geometrical difference of concern is the location of the western (left) side of the model area, where the model domain used in the present study is consciously expanded to the west in order to fully capture the sink capacity of the Vättern Lake as well as to put the Comparison Site a little further away from the model boundary. The maximum water depth of the Vättern Lake is c 120 m, which means that its deepest bathymetry is c 30 m below the Baltic Sea. The bathymetry is illustrated in Figure 1-3.

The right image of Figure 2-3 shows the major drainage basins in southern Sweden. The arrows indicate the regional runoff directions for Östra Götaland. By comparing the two images of Figure 2-3 it is noted that the Comparison Site is located at the main surface water divide between the drainage area of the Vättern Lake and the drainage area of the Emån Stream. The drainage area of the Vättern Lake in the northwest part covers c 30% of the terrestrial model area. The surface water runoff direction is to the north before it eventually discharges into the Baltic Sea at the rim of the northern boundary. Approximately 30% of the surface water runoff discharges through the western and southern boundaries. Hence, c 40% of the surface water runoff of Östra Götaland discharges to the eastern shoreline.

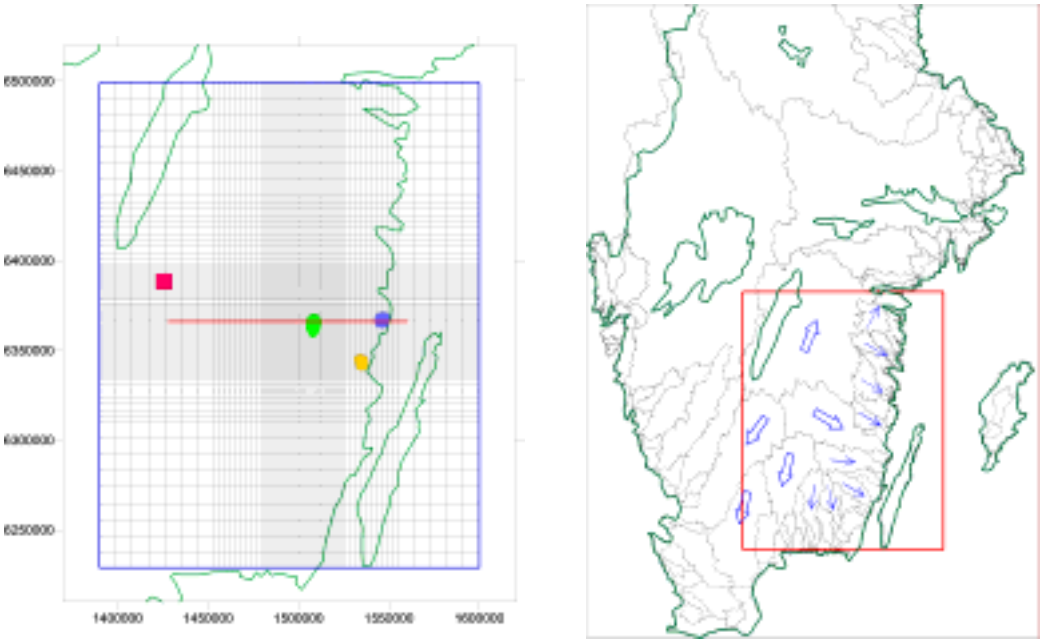

Figure 2-3. *Left. The mesh used to mimic the mesh shown in Figure 2-2. The locations of the four exploratory sites; red = the Comparison Site, green = Hultsfred Östra, yellow = Oskarshamn Södra and blue = Simpevarp. The topographic variations along the red line are in shown in Figure 2-4 and Figure 2-5. Right: Major drainage basins in southern Sweden. The arrows indicate the regional runoff directions for Östra Götaland.*

Hydrogeological properties vary a lot between different geological formations. In addition, most geological formations show spatial variability in their hydrogeological properties. This is particularly true for the geology of Östra Götaland, which by and large consists of sparsely fractured crystalline rock under a thin cover of glacial till. However, the study is not focusing on the role of geological features such as fractures, fracture zones, clay layers and glaciofluvial deposits, which all bring complexity to the permeability field in terms of heterogeneity and anisotropy. Due to a high net precipitation in combination with rather low permeabilities of both the crystalline rock and the till, which is by large the dominating Quaternary deposit, the groundwater table is in most places close to the ground surface and follows the local variations of the topography more or less. In conclusion, the topography is an important factor for both surface water and groundwater runoff. The question treated here is to what extent the regional and local surface water divides affect the groundwater flow pattern at depth assuming a homogeneous and isotropic porous medium of low permeability.

/Voss and Provost, 2001/ used land-surface elevation data obtained from /LMV, 2000/ on a grid of 500 m. The same elevation database was used in the present study. A major difference between the two studies is in the mesh discretisation, which affects the resolution of the local topographic variations. The differences are visualised in Figure 1-2 and Figure 1-3. Voss and Provost commented that the mesh in Figure 2-2, which is compatible with that shown in Figure 1-2, must be considered a rather coarse discretisation of the region and the results should not be seen as uniformly accurate. In a way the present study can be regarded as a follow-up study to Voss and Provost's wish to use a much finer mesh with more regular areal discretisation.

As a means of assessing the impact of different mesh discretisations on the representation of local topographic gradients, the land-surface elevation data on a 50 m grid /LMV, 2000/ was plotted for the red line shown in the left image of Figure 2-3. The elevation data are shown in Figure 2-4 together with the linear regression, the gradient of which is c 0.2%. As shown in Figure 2-4 the local topography varies a lot along the profile.

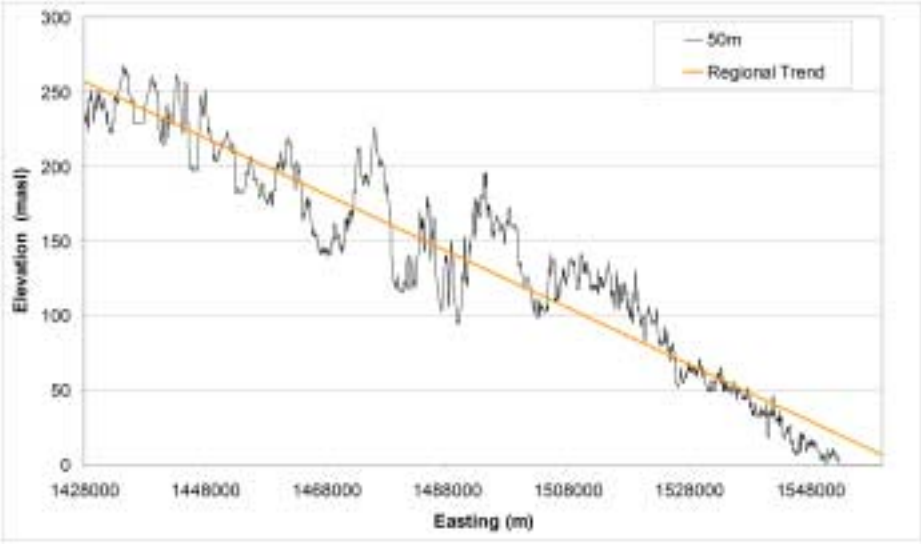

Figure 2-4. *The linear regional linear gradient is c 0.2% along the red line in Figure 2-3. The local topography varies a lot along the profile.*

The upper image of Figure 2-5 shows local topographic gradients along the red line. On this scale (50 m) the local gradients can be up to 100 times greater than the linear regional gradient shown in Figure 2-4. The median value of the stepwise 50 m gradients is c 3.3%, which is about ten times greater than the linear regional gradient shown in Figure 2-4. The lower image of Figure 2-5 shows approximate model gradients along the red line in Figure 2-3 for three different mesh discretisations, 500 m, 1 500 m and 5 000 m. The median values of the stepwise 500 m gradient, 1 500 m gradient and 5 000 m gradient are c 1.3%, 0.6% and 0.3%, respectively. In conclusion, the aforementioned concern of Voss and Provost about the impact of the chosen mesh discretisation on their simulation results is well founded. Indeed, a mesh discretisation of 500 m is on the same order of magnitude as the considered depth in the Swedish KBS-3 programme. Without doubt the occurrence of local flow cells in the numerical modelling is likely to be highly dependent on the chosen resolution of the mesh discretisation.

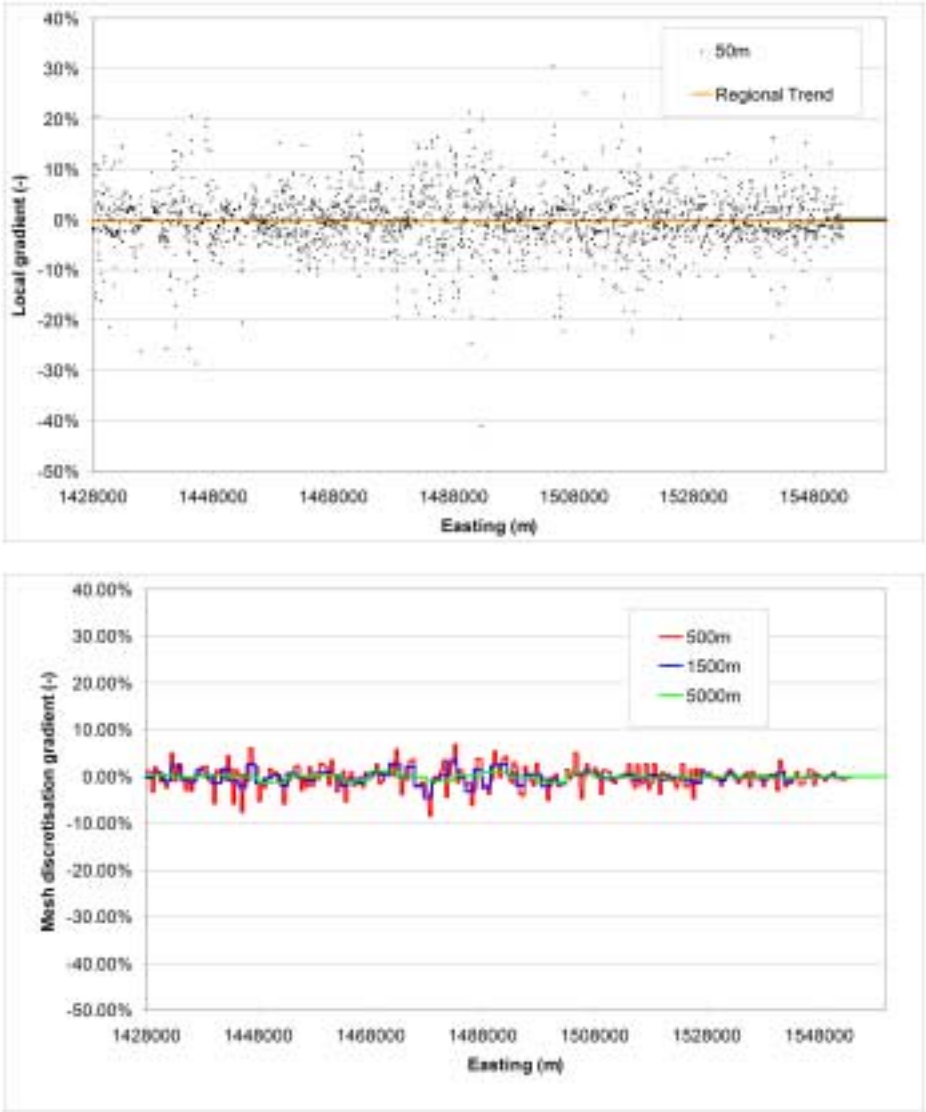

Figure 2-5. *Top: Local topographic gradients along the red line in Figure 2-3 based on elevation data on a 50 m grid. Bottom: Approximate gradients along the red line in Figure 2-3 for three different mesh discretisations, 500 m, 1 500m and 5 000 m.*

Voss and Provost used a 10 km deep variable-density flow model in combination with the topography in their study of regional flow cells. The model domain consisted of 15 layers; 4×250 m layers, 4×500 m layers and 7×1 000 m layers, see the left image of Figure 2-6. The right image of the same figure visualises the mesh discretisation of the replicate model used in this study. The model domain used by Voss and Provost consists of c 56 000 cells and the replicate model c 70 000 cells. The difference is due to the aforementioned extension of the western boundary in the replicate model.

The refined mesh discretisation model used to grasp the 500 m topography and bathymetry shown in Figure 1-3 consists of 540 rows, 420 columns and 22 layers, which altogether yield c five million cells. The increased number of layers is required in order to capture the near-surface groundwater flow. The refined mesh discretisation in the vertical direction is as follows (metres): 30, 50, 70, 7×100, 200, 450, 500, and 7×1 000.

/Tóth, 1963/ presented an instructive image on recharge and discharge, which shows how a change in the relative strength between local and regional topographic gradients affects the presence of local flow cells at depth. The image is repeated in Figure 2-7. The ratio between the vertical and the horizontal length scales is close to 1:20, which lends itself to interesting comparisons with the model domain of Östra Götaland, which is 210 km wide and 10 km deep, cf Figure 2-6.

The regional topographic gradient shown in Figure 2-7 is 10%. In the upper image the maximum local topographic gradient is c 4%, whereas in the lower image it is c 16%. Thus, the ratio between the local and regional gradients is 0.4 and 1.6, respectively. For Östra Götaland the maximum regional topographic gradient is c 0.35%. The values of the median of the stepwise 500 m, 1 500 m and 5 000 m local gradients are c 1.3%, 0.6% and 0.3%, respectively, which render local-to-regional gradient ratios of c 4, 1.7 and 0.8, respectively, for the three mesh discretisations of Östra Götaland.

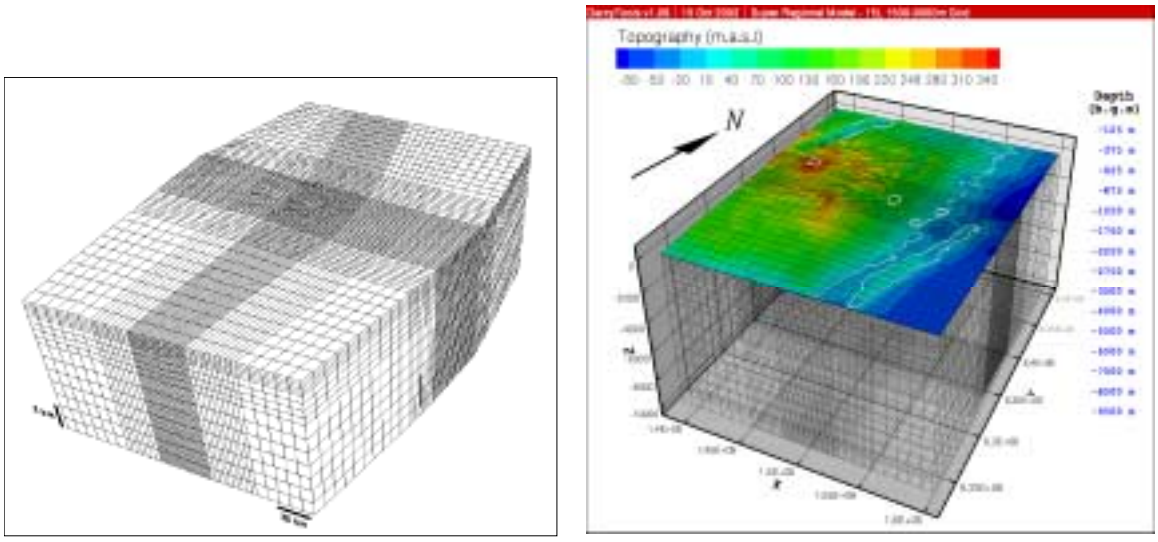

Figure 2-6. *Left: Oblique view of the model mesh used by /Voss and Provost, 2001/. Right: Transparent view of replicate model mesh used in this study. The three-dimensional mesh is exaggerated circa ten times in the vertical direction.*

The studied local-to-regional gradients for Östra Götaland are as great or greater than the ones shown in Figure 2-7, however, the local-to-regional gradient ratio is not the only mechanism that affects the depth of local flow cells. /Zijl, 1999/ concluded that the 'depth' of a flow cell is a complex entity, which is a function of, among other things, the wavelength of the spatial variability in the topography. The wavelength of the local variations is fixed for the two cases shown in Figure 2-7; whereas it varies for Östra Götaland, cf Figure 2-4. The ratio between the wavelength and the depth of the model domain is much greater in Figure 2-7 than for Östra Götaland, which impede a direct comparison.

However, by taking groundwater salinity into account for Östra Götaland, the likelihood for short distances between recharge and discharge areas affecting groundwater flow at 500 m depth will increase dramatically due to the contrast in fluid density. That is, the density contrast effectively decreases the depth of the freshwater flow system. According to the borehole measurements at Laxemar, which is located close to Simepvarp, the salinity is estimated to c 10% at 2 000 m depth /Rhén et al, 1997/.

The above analysis is somewhat speculative. However, the point made here is that the local topographic gradients of Östra Götaland are strongly indicative of local flow cells and that the result of numerical modelling is likely to be dependent on the chosen resolution of the mesh discretisation. On top of this lies the hydrogeological fact that the fabric is not porous but consists of fractured crystalline rock, which is highly anisotropic. An important factor associated with the occurrence of vertical fractures zones, however, is that the majority of these occur in valleys, hence strengthening the pattern of local flow cells. This important fact is also overlooked by Voss and Provost, who treated anisotropy as a uniformly distributed entity, which is not consistent with field data.

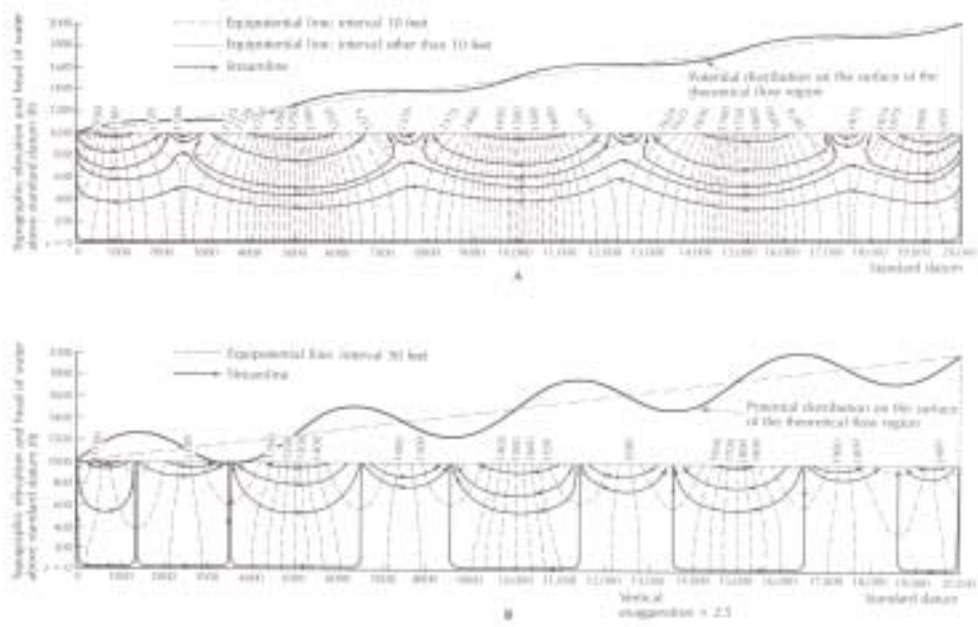

Figure 2-7. *A reproduction from /Tóth, 1963/, which shows how the strength of local topographic gradients with regards to the regional topographic gradient affects the relation between the local and regional flow cells. The ratio between the vertical and the horizontal length scales is approximately 1:20.*

3 Model setup

3.1 Modelling of boundary conditions and physical processes

The model setup mimics the model setup used by Voss and Provost. Figure 3-1 illustrates a schematic cross section through the model domain from west to east together with the boundary conditions and processes used in both studies. The model mesh follows the bathymetry of the Vättern Lake and the Baltic Sea, whereas all other surface water bodies are modelled as land surface as given by the elevation database.

The reader is referred to /p 27 of Voss and Provost, 2001/ for a detailed description of the no-flow boundary conditions and the "salt generator". From a hydrogeological point of view, we would like to bring the reader's attention to two issues, the effects of which are not clear from the report by Voss and Provost. First, the no-flow boundary conditions in the southwest effectively reroutes the natural regional runoff towards the eastern shoreline, thus causing an unrealistic regional flow pattern in this part o the model domain. This approximation may be advocated to be insignificant for the flow below the four exploratory sites, which are located more or less in the centre of the model domain. However, such a rationale is not tested by Voss and Provost by means of a sensitivity study. The true runoff directions can be grasped in the right image of Figure 2-3. The boundary conditions on the other sides of the model domain are less ambiguous from a hydrogeological point of view, although their impact are not tested either.

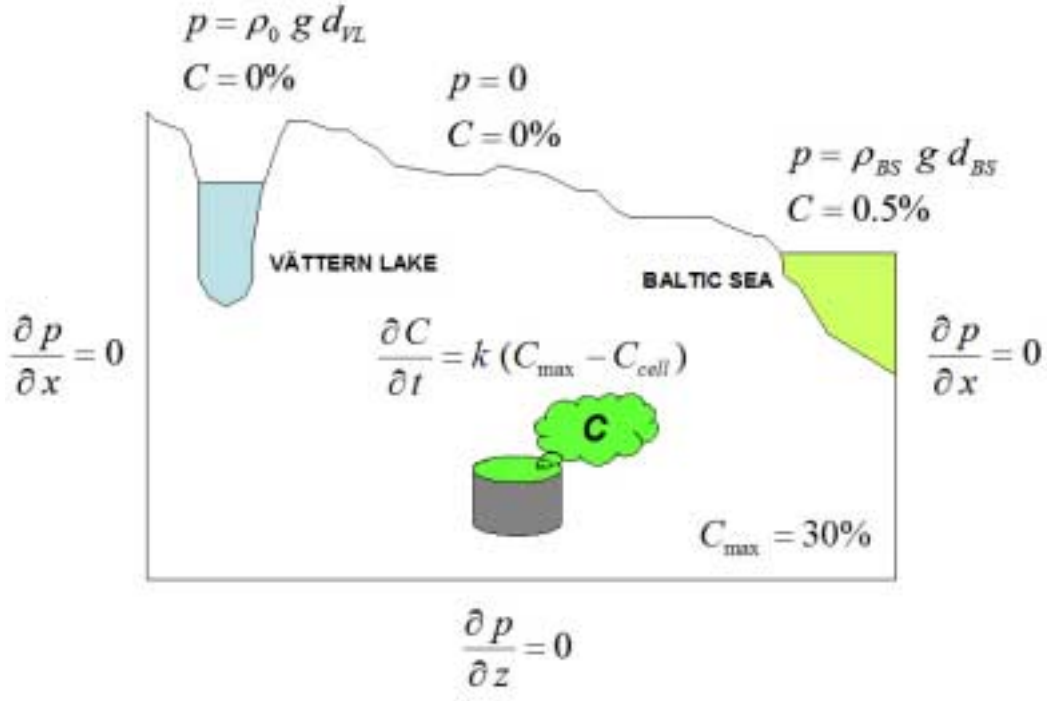

Figure 3-1. *Boundary conditions and processes used in the present study.*

Second, the ‘salt generator’ shown in Figure 3-1 suppresses mixing by advection as the main mechanism for explaining the groundwater chemistry, an assumption that is not obvious given the research results presented by /Laaksoharju, 1999/. Moreover, the mass transfer coefficient k, which is a rate constant for the production of salt, has a very long time scale. The value of k used for the isotropic case mimicked here is $4.5 \cdot 10^{-15}$ s^{-1}, which renders that c 6–7 Ma are required in order to alter the salinity by 1% at depth assuming no advection. Closer to land surface c 1–1.5 Ma are needed. The implication of the ´salt generator’ is that the simulation time needed to reach a steady-state flow and solute concentration becomes extremely sensitive to the initial condition of salinity.

Voss and Provost stated that they simulated a steady-state flow and solute concentration to represent present-day conditions, and that the repository siting was then evaluated on the basis of this flow field. The amount of time elapsed in the present interglacial, i.e. c 14 ka, may be sufficient to reach a steady state, see e.g. /Provost et al, 1998/ and /Follin and Svensson, 2002/. However, given the strong impact of the ongoing rebound process, see e.g. /Voss and Andersson, 1993/, a word of caution about the present-day conditions being at a steady state seems logical. The shoreline displacement process is expected to alter the topography of Östra Götaland by c 15 m within the next 10 ka /Påsse, 1996/.

3.2 Model input data

The boundary conditions together with the permeability and flow porosity fields govern the flow pattern and salinity distribution of a steady-state flow and solute concentration model. For the particular case studied here we used the model input data setup that Voss and Provost’s refer to as ‘three mutually perpendicular fracture sets of equal spacing and properties throughout the bedrock’. The data set used is denoted Case 1:1 in Table 2, p 29 in /Voss and Provost, 2001/. The permeability and flow porosity fields of Case 1:1 are homogeneous and isotropic, the values of which were set to $1.02 \cdot 10^{-16}$ m^2 and 0.1%, respectively.

3.3 Computer code

The simulations were run using the computer code DarcyTools /Svensson et al, 2002/, which is based on a finite-volume formulation of the governing equations for mass and salt conservation. Pressure and salinity were solved fully coupled using a multi-grid solver.

4 Results of 3D modelling

4.1 Code verification

Voss and Provost based their 3D modelling on the "Recharge Area Concept", an approach which was first introduced by /Tóth and Sheng, 1994/. Inspired by /Tóth and Sheng, 1996/, Voss and Provost used a numerical technique to calculate so called return-flow times for the visualisation of their model results. Return-flow times are calculated by reversing the flow field (through the boundary conditions) and specifying a constant, uniform production of "solute", the concentration of which represents groundwater age, with a concentration of zero at recharge. A zero-order solute production of one per year is used.

In the present study we used traditional particle tracking to visualise the model results. As a means of convincing ourselves (and the reader) that the functionality of the computer code used here is compatible with the computer code used by Voss and Provost, one of the test cases run by Voss and Provost was also run in the present study using the return-flow technique described above. The particular test case is specified on /p 8 of Voss and Provost, 2001/ and the reader is kindly referred to this reference for a detailed specification of the model setup. The result reported by Voss and Provost is shown in the left image of Figure 4-1. The right image shows the result obtained in the present study.

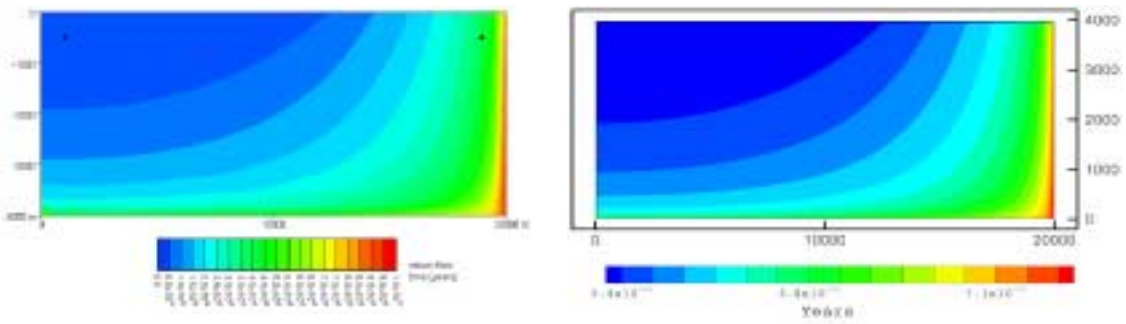

Figure 4-1. *Visualisation of return-flow times for the code verification test case. Left: Figure 1 of /Voss and Provost, 2001/. Right: This study.*

Another example of code verification is given in Appendix A, which presents simulation results from a comparison between the computer code used to study the regional-scale groundwater flow pattern in Northern Uppland /Holmen et al, 2003/ and the computer code used in the present study. Appendix A reveals that the two codes give identical results for the problem studied.

4.2 Mesh discretisation – Model A and Model B

In what follows, the replicate model, which mimics the mesh discretisation used by Voss and Provost, is referred to as 'Model A' and the refined mesh discretisation model as 'Model B'. The representation of the topography of Östra Götaland using the two mesh discretisations is shown in Figure 4-2.

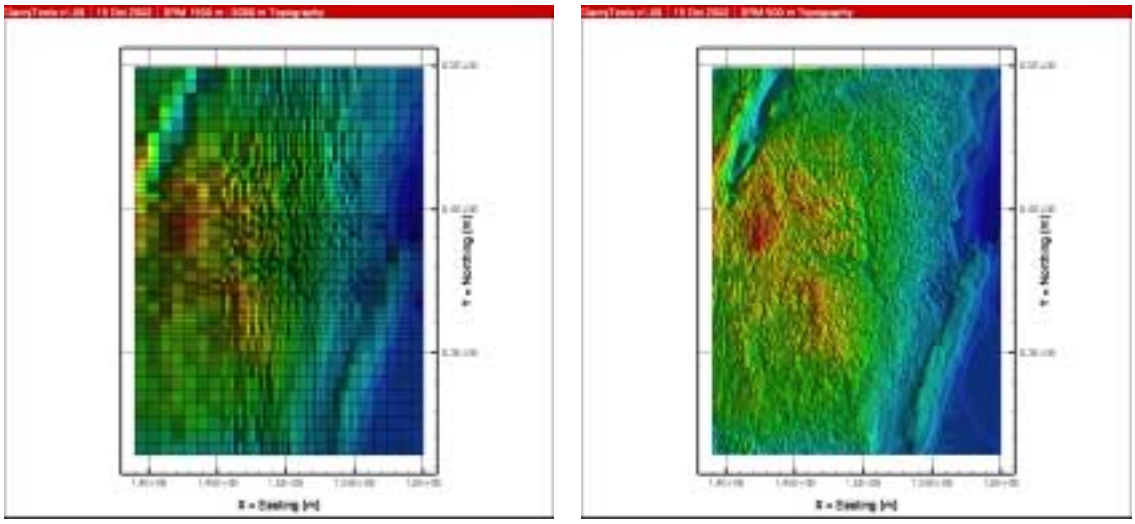

Figure 4-2. *Visualisation of the mesh discretisation of Model A (left) and B (right).*

4.3 On the role of the initial condition of salinity

Since salinity is accounted for in the model setup and salt is generated, it is important to understand the role of the initial condition of the salinity field on the simulation results. The initial condition used by Voss and Provost is not explained in their report, but according to /Voss, 2002, personal communications/ Voss and Provost started with a linear salinity gradient.

Due to the large number of cells for Model B (c 5 million) comparisons with Model A results were made at two time slices, 40 ka and 110 ka. Model A was run to 500 ka with one intermediate analysis at 225 ka.

Figure 4-3 shows two iso-surfaces of the salinity field, 0.1% and 7%, at three different time slices, 40 ka, 110 ka and 500 ka, using Model A. According the three time slices shown in Figure 4-3, it takes a long time to reach a near steady-state flow and solute concentration, which was the case simulated according to Voss and Provost. The time needed to reach a steady state is not stated in their report, however. By comparing the differences between different time slices, 40 ka, 110 ka, 225 ka, and 500 ka we found that the differences between 225 ka and 500 ka using Model A to be relatively small with regards to changes in salinity field and in the Darcy velocity field.

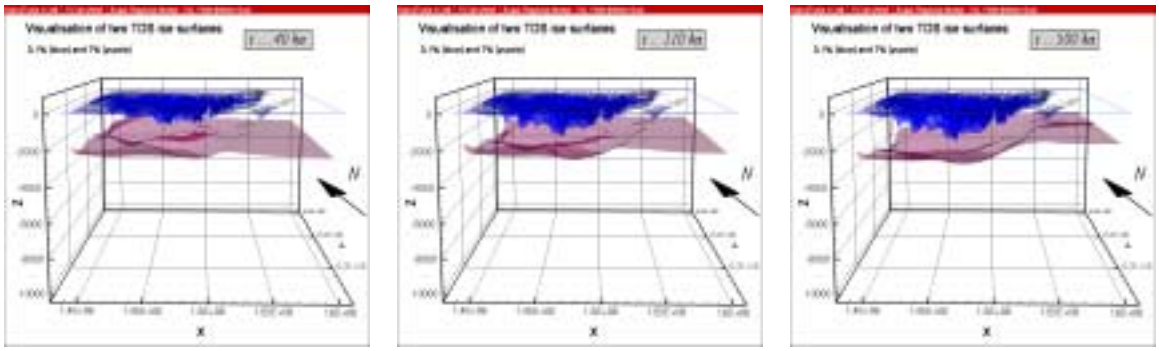

Figure 4-3. *Visualisation of two iso-surfaces of the salinity field at different time slices using Model A.*

4.4 On the role of mesh discretisation

The role of the mesh discretisation is visualised in Figure 4-4, which shows two-colour maps of the vertical component of the Darcy velocity field for Model A and B at a time slice of 40 ka. In Figure 4-4, grey means downward movement and olive green upward. The impact of the mesh discretisation is remarkable. Model A renders much less flow cells, a distorted distribution of recharge and discharge areas at all elevations throught the model domain including land surface and an exaggerated penetration depth.

In Section 4.4.1 we analyse these differences between the two results shown in Figure 4-4 and present particle tracking results for the Comparison site. Section 4.4.2 contains particle tracking results for Hultsfred Östra. Particle tracking results for Oskarshamn Södra and Simpevarp are not treated in detail, but an approximate study is found in Appendix A, which presents a comparison between the computer code used to study the regional-scale groundwater flow pattern in Northern Uppland /Holmén et al, 2003/ and the computer code used in the present study. The comparison in Appendix A was made for a constant-density fluid formulation of the mass conservation and a regular mesh discretisation of 330 m. The depth of the flow model was set to 1 100 m.

4.4.1 Comparison site

The Comparison Site is located at the crest of the southern Swedish highlands, c 350 m a s l. Figure 4-5 shows simulation results at 40 ka using Model A. The four images of Figure 4-5 show the vertical component of the Darcy velocity field at different depths; –1 250 m, –2 250 m, –3 500 m and –6 500 m. Also shown are the pathways of 342 particles released below the Comparison site at repository depth using a particle spacing of 500 m. The resolution of the Darcy velocity field observed close to land surface vanishes entirely at depth. The downward movement of the salinity field captures a substantial portion of the particles and brings them to the eastern shoreline where they discharge into the Baltic Sea. However, for the considered time slice of 40 ka the body of the tracked particles discharges nearby the Comparison site or into the Vättern Lake.

Figure 4-6 shows simulation results for Model A at four different time slices; 40 ka, 110 ka, 225 ka and 500 ka. The chosen XY-planes for the vertical component of the Darcy velocity field coincide roughly with the maximum penetration depth at each time slice. The spreading of the particles at early time slices is due to the transients caused by the initial condition of salinity, cf Figure 4-3. The results in Figure 4-6 show that 40 ka as well as 110 ka are insufficient as time slices in order to advocate that a near steady-state flow and solute concentration have been reached. In our opinion, the results presented by Voss and Provost look a lot like those for the 110 ka time slice, or perhaps even the 40 ka time slice, thus implying not only an insufficient mesh discretisation but also an insufficient simulation time.

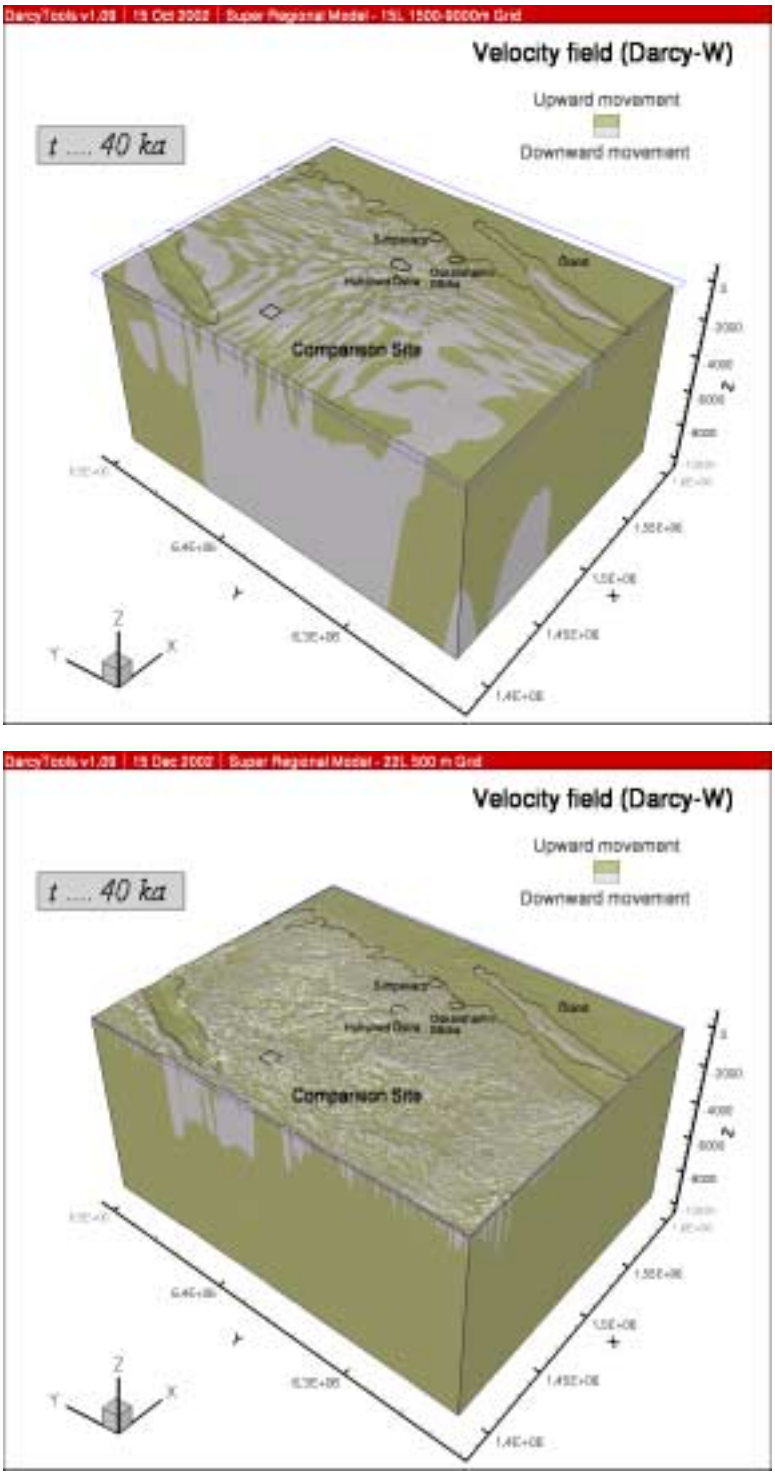

Figure 4-4. *Two-colour maps showing the sign of the vertical component of the Darcy velocity vector for Model A (left) and B (right) at a time slice of 40 ka. Grey means downward movement and olive green upward.*

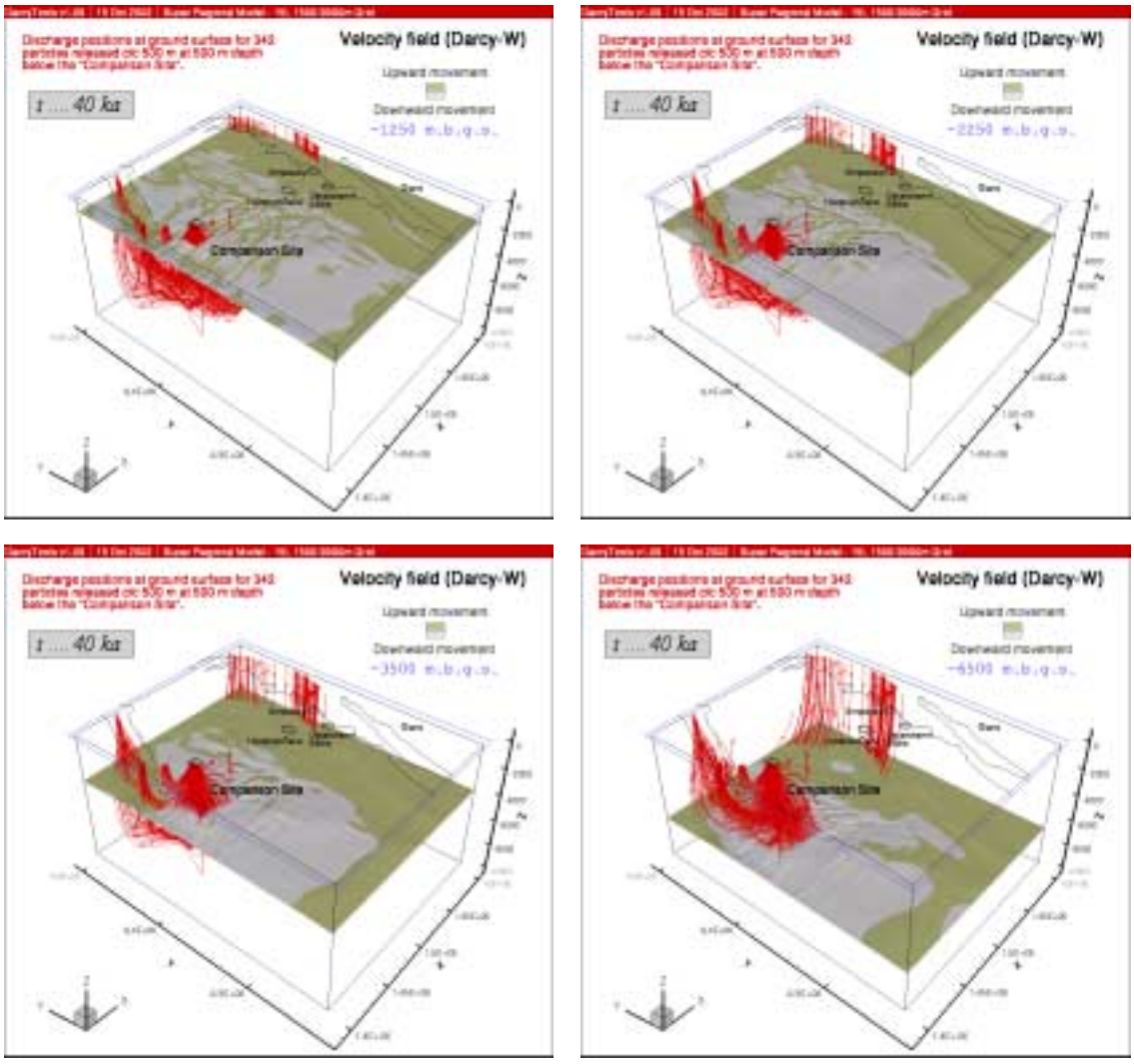

Figure 4-5. *Simulation results at a time slice of 40 ka using Model A. The four images shows the vertical component of the Darcy velocity field at different depths; –1 250 m, –2 250 m, –3 500 m and –6 500 m. Also shown are the pathways of 342 particles released below the Comparison site at repository depth using a particle spacing of 500 m.*

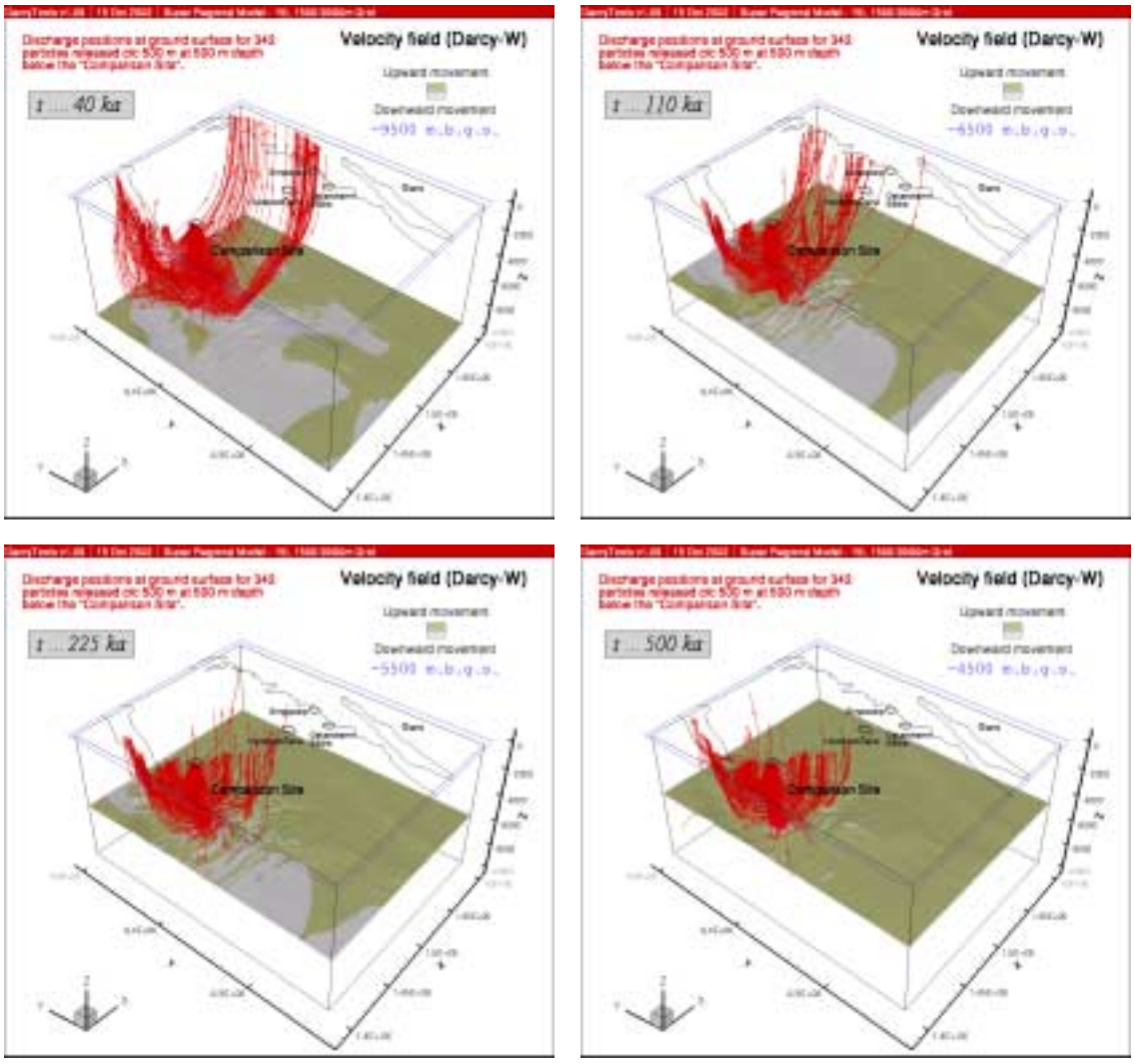

Figure 4-6. *Simulation results for Model A at four different time slices; 40 ka, 110 ka, 225 ka and 500 ka. The chosen XY-planes showing the vertical component of the Darcy velocity field coincide roughly with the maximum penetration depth at each time slice.*

The left column of images in Figure 4-7 shows the same pathways as shown in Figure 4-6 excluding the XY-planes showing the vertical component of the Darcy velocity field. The right column of images shows the same particle pathways in plane view.

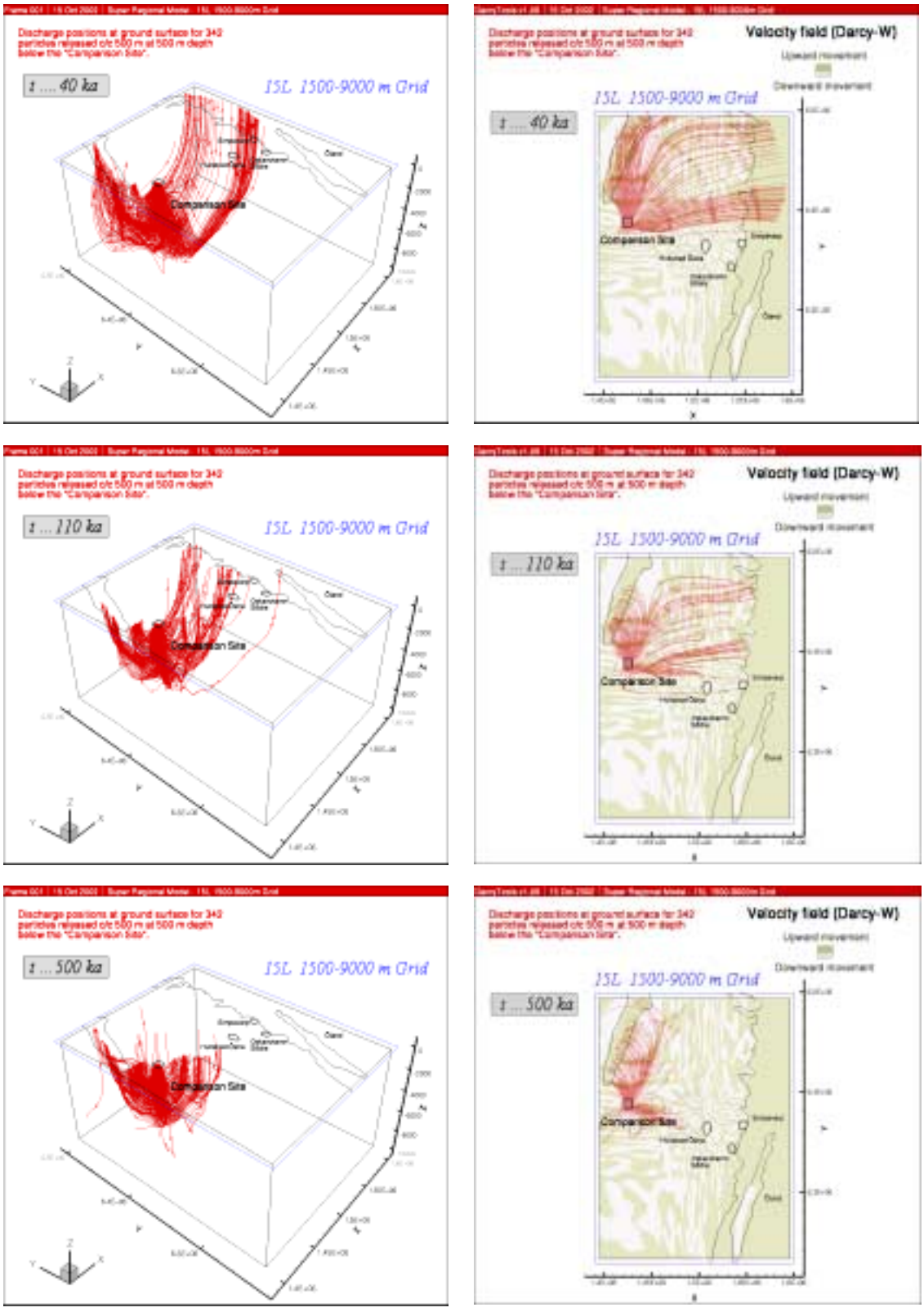

Figure 4-7. *Left: The same pathways as shown in Figure 4-6 excluding the XY-planes showing the vertical component of the Darcy velocity field. Right: The same pathways shown in plane view.*

Figure 4-8 allows for comparisons between Model A and B results at two time slices, 40 ka and 110 ka. Model A results are shown to the left and Model B results to the right. The starting positions of the released particles are identical, yet the differences in the tracked pathways are significant. The results for the two time slices using Model B are a lot more alike than for Model A, thus implying a better solution all together using a finer mesh discretisation.

The pathways for Model B in Figure 4-8 indicate that the vast majority of the released particles discharges in the vicinity of the 'repository area' or at the shoreline of the nearby Vättern Lake, thus suggesting that a finer mesh discretisation maintains the impact of the local topographic gradients down to a considerable depth beneath the Comparison site. This interpretation is confirmed by Figure 4-9, which shows the vertical component of the Darcy velocity field at 500 m depth below land surface using Model B results at a time slice of 110 ka.

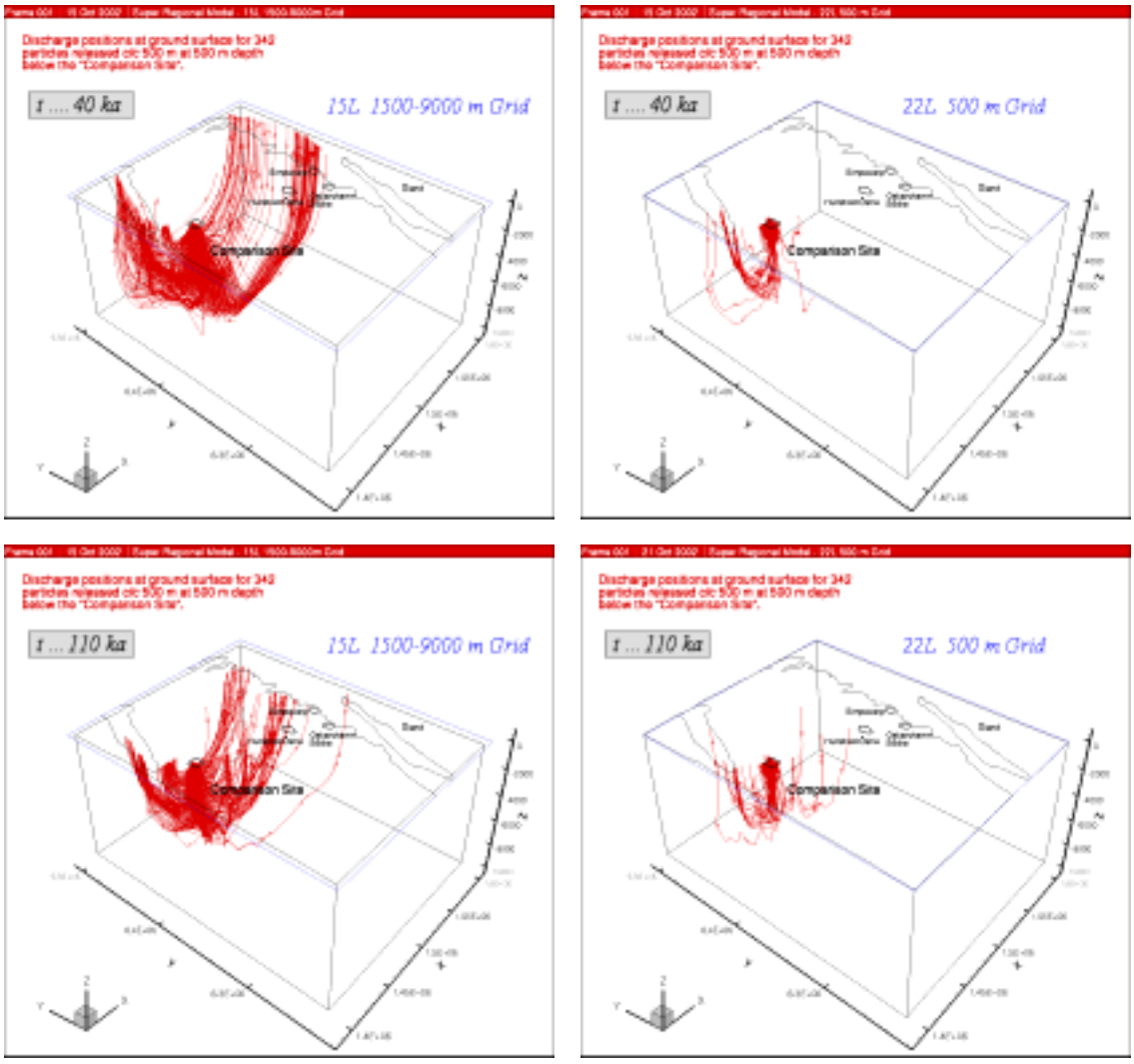

Figure 4-8. *Comparison between Model A and B results at two time slices, 40 ka and 110 ka. Left: Model A results. Right: Model B results.*

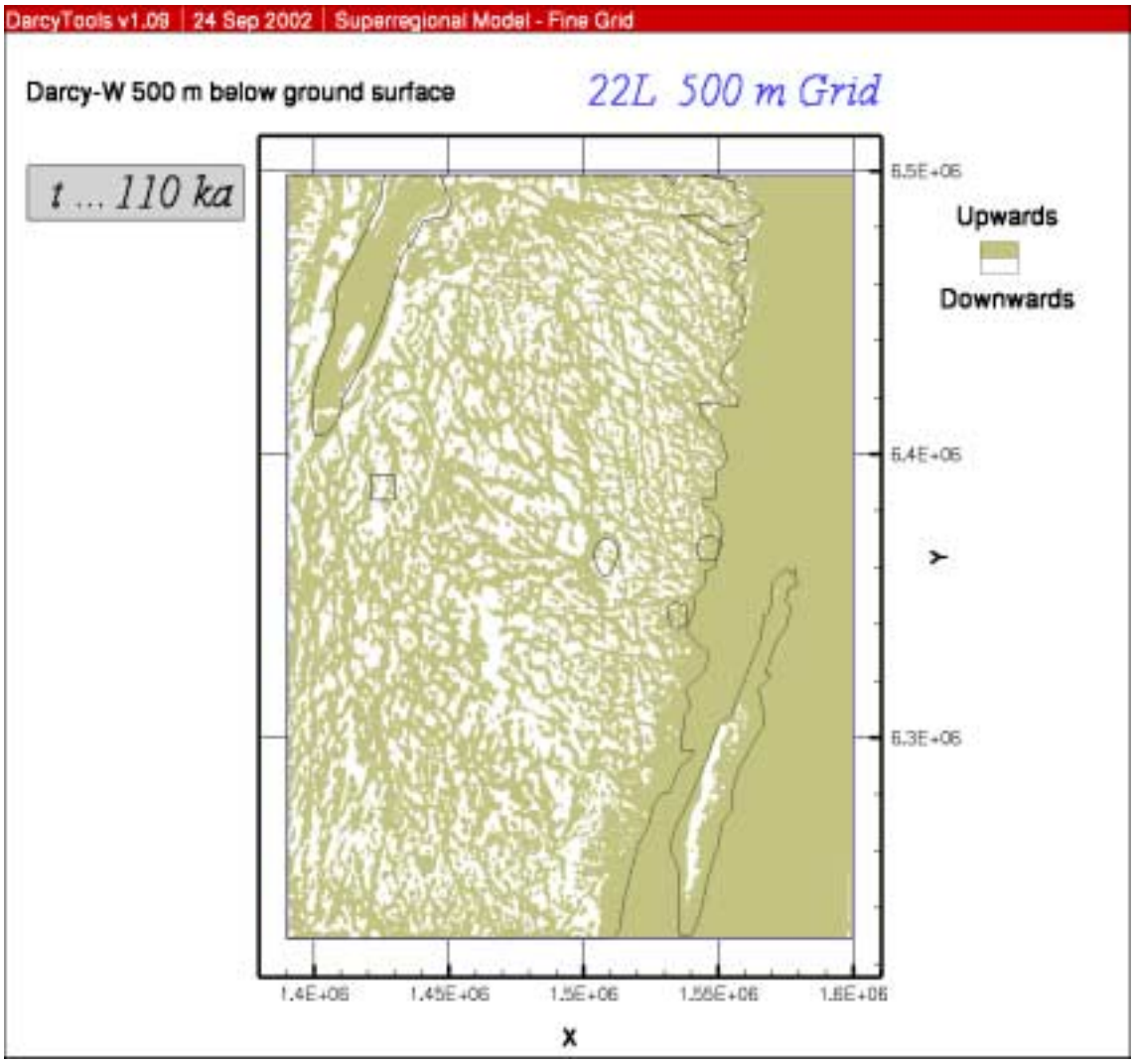

Figure 4-9. *The vertical component of the Darcy velocity field at 500 m below land surface using Model B results at a time slice of 110 ka.*

The four images of Figure 4-8 are shown in plane view in Figure 4-10 emphasising the indications stated previously. Model A results are shown to the left and Model B results to the right.

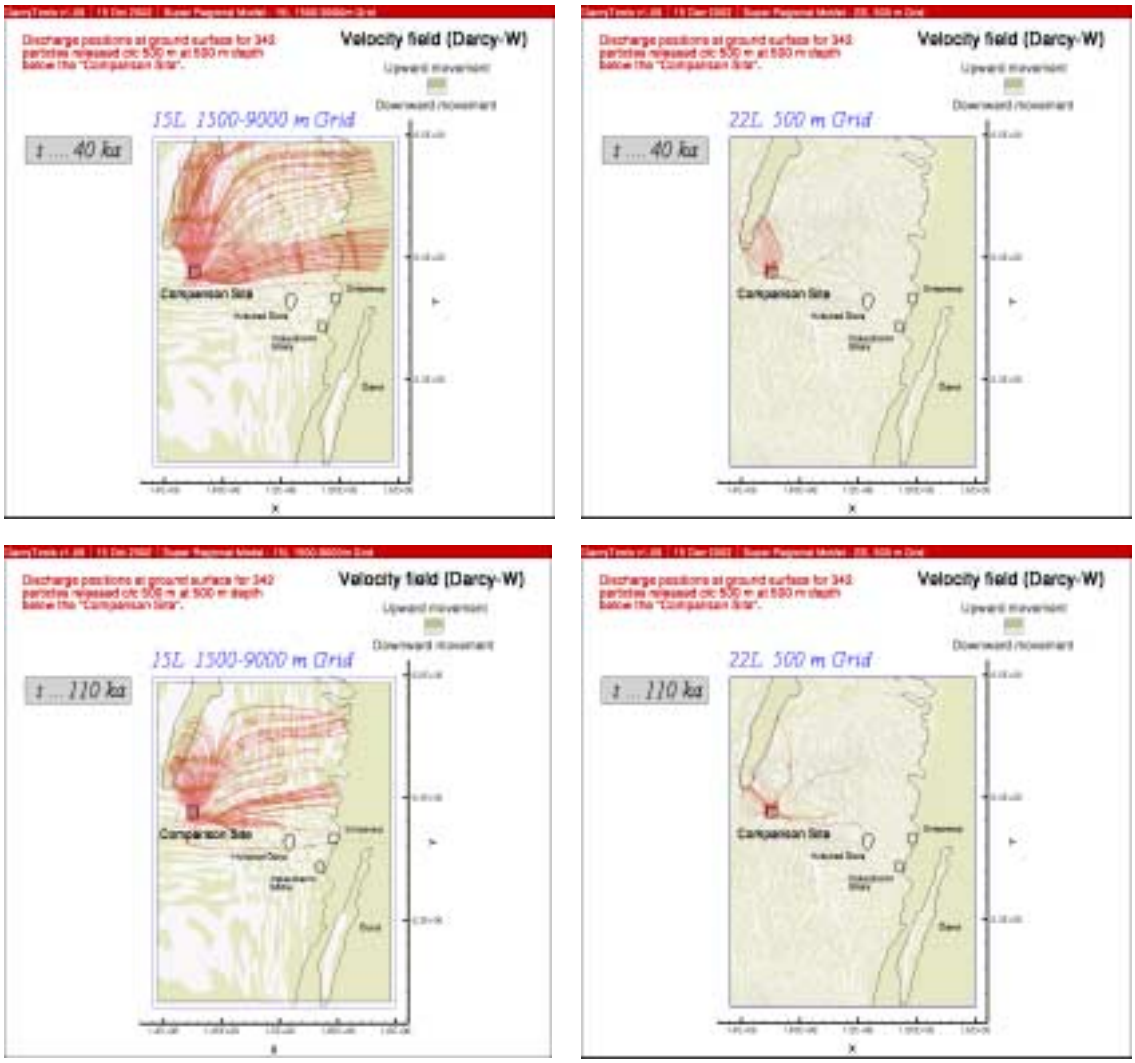

Figure 4-10. *Plane view of the four images of Figure 4-8. Left: Model A results. Right: Model B results.*

4.4.2 Hultsfred Östra

Hultsfred Östra is located on the surface water divide between the drainage area of the Emån Stream and the drainage area of the streams flowing north of Oskarshamn towards the Simpevarp area, e.g. the Laxemar Stream and the Mistra Stream. The location is visualised in Appendix A, Figure A-1. The maximum elevation of Hultsfred Östra is c 140 m a s l, cf Figure 2-4.

The top and centre images of Figure 4-11 are close-ups of Figure 4-4 showing the vertical component of the Darcy velocity field close to the three exploratory sites Hultsfred Östra, Oskarshamn Södra and Simpevarp. The lower close-up image visualises the refined mesh discretisation of Model B. Note the depth of local flow cells at the edge of the model domain.

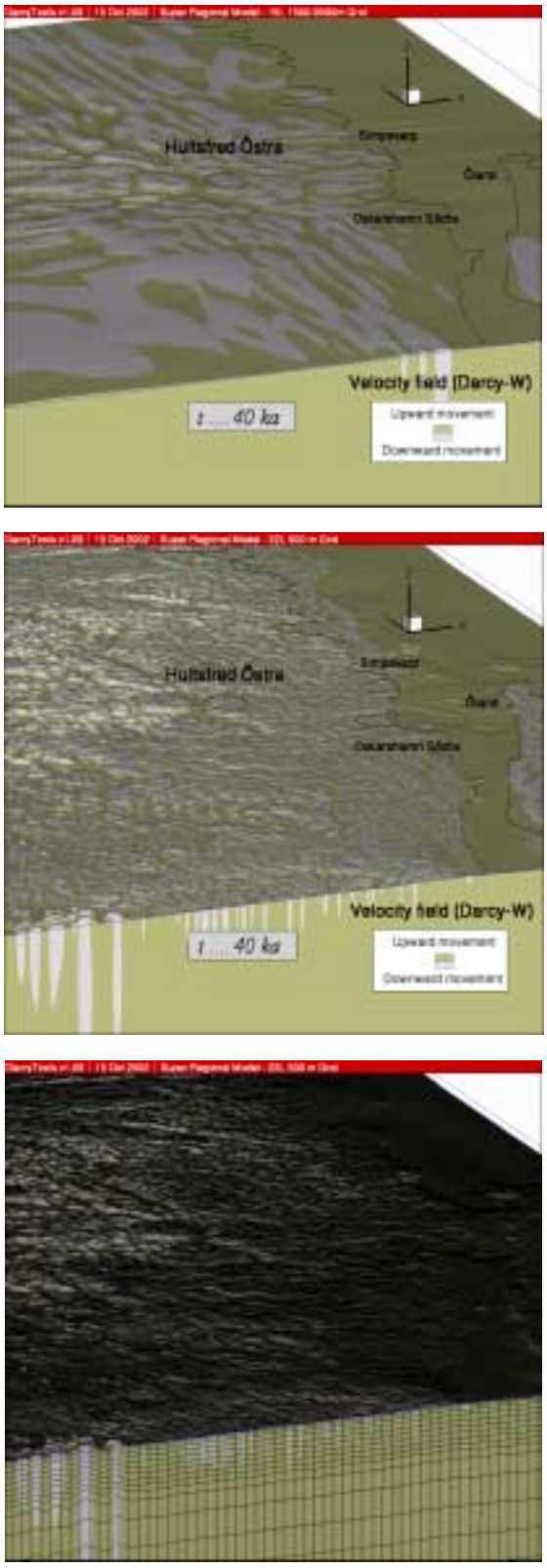

Figure 4-11. *Top and centre: Close-up images of Figure 4-4 showing the vertical component of the Darcy velocity field at the three exploratory sites Hultsfred Östra, Oskarshamn Södra and Simpevarp. Bottom: Close-up image showing the refined mesh discretisation of Model B.*

Figure 4-12 shows results at 40 ka using Model A (left) and B (right). The upper images show the vertical component of the Darcy velocity field at repository depth together with the pathways of 504 particles released 500 m below Hultsfred Östra. The lower images shows the pathways solely. Approximately 90% of the particles released in Model A discharge to the land surface in the immediate vicinity of their starting positions. The corresponding number of particles for Model B is c 93%. Hence, the vast majority of the particles released at Hultsfred Östra are not captured by a regional flow field, but discharges more or less according to the local topographic gradients.

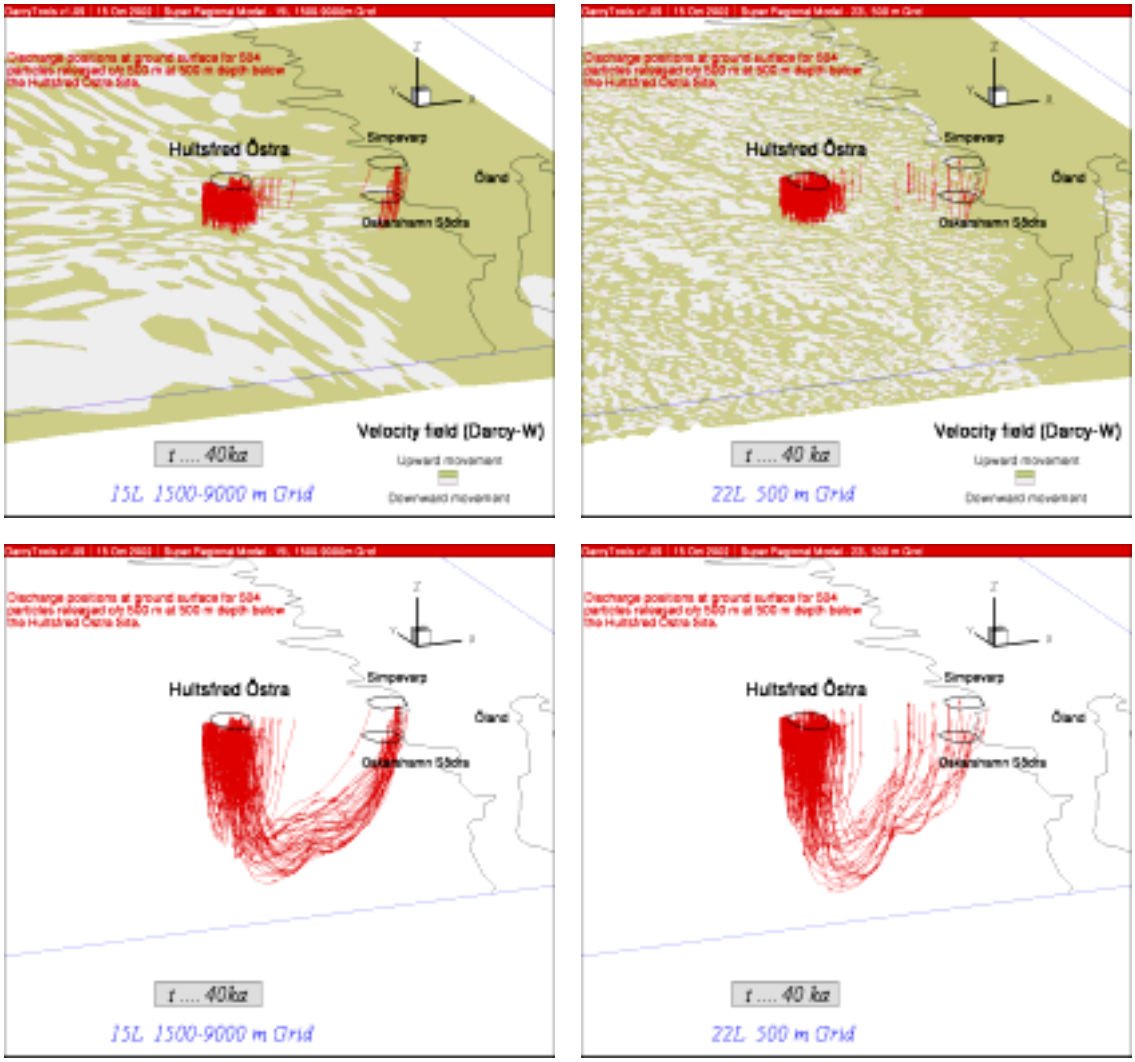

Figure 4-12. *Simulation results for Hultsfred Östra at 40 ka using Model A (left) and B (right). The upper two images show the vertical component of the Darcy velocity field at repository depth together with the pathways of 504 particles released 500 m below Hultsfred Östra using a particle spacing of 500 m. The lower two images show the pathways solely.*

The differences between the Model A and B results for Hultsfred Östra are less than between the Model A and B results for the Comparative Site. This is probably due to the smaller difference in the mesh discretisations between Model A and B for the Hultsfred Östra case. Other important factors also supporting a better agreement between Model A and B results for Hultsfred Östra are the closeness to the shoreline and the subsequently smaller depth to the interface between fresh and saline groundwater.

Figure 4-13 suggests that the simulation results of Model A at the time slices 40 ka and 110 ka are less accurate than that of Model B at 40 ka. That is, the results of Model A at a time slice of 500 ka are much closer to that of Model B at 40 ka. This result supports the aforementioned indication that Voss and Provost besides an insufficient mesh discretisation may also have used an insufficient simulation time given the initial condition of the salinity field.

Figure 4-14 shows both a perspective view and a plane view of the particle pathways and their discharge locations using Model B at a time slice of 40 ka.

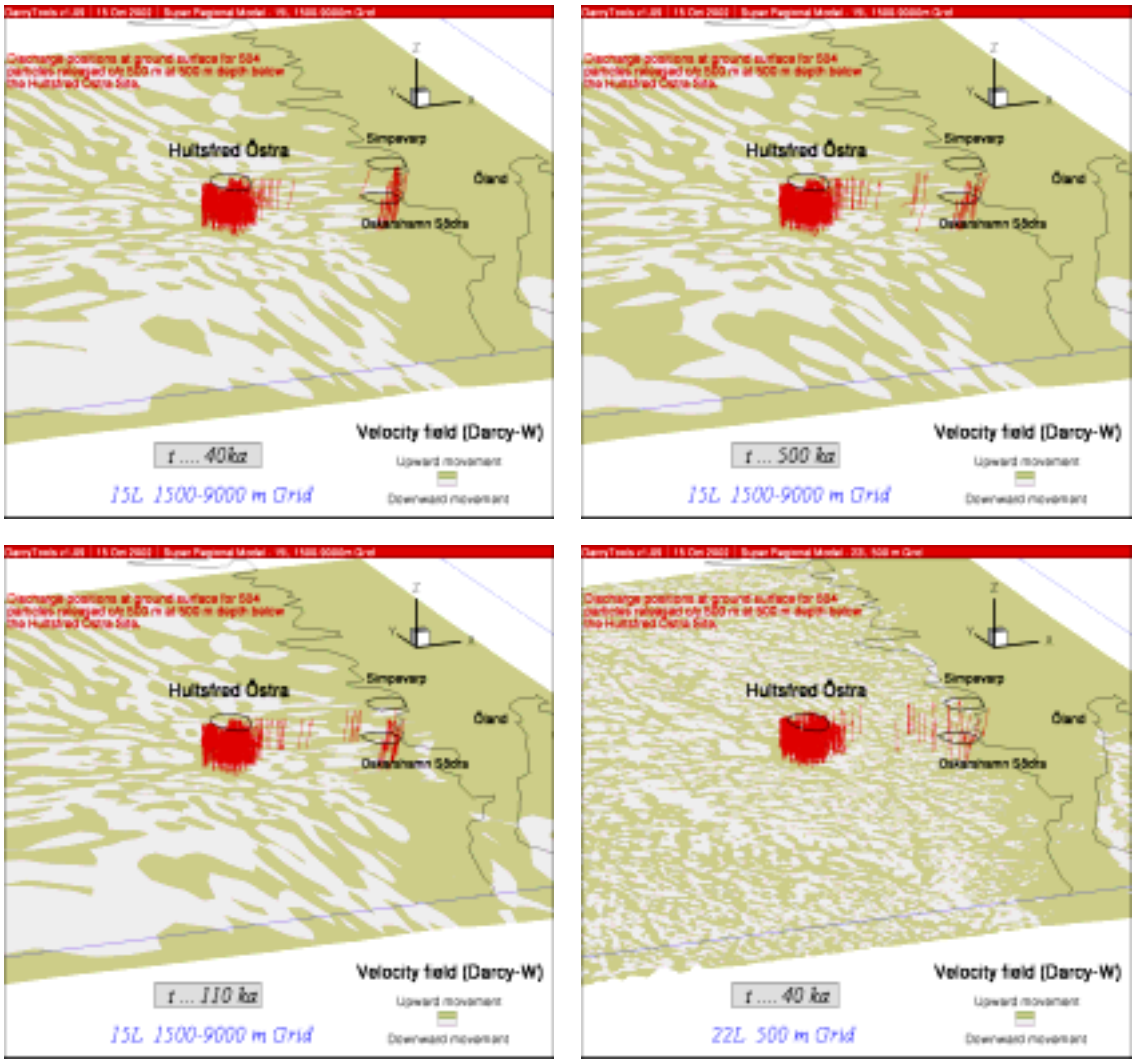

Figure 4-13. *The simulation results for Model A at a time slice of 500 ka are closer to that of Model B at 40 ka than the Model A results at 40 ka and 110 ka.*

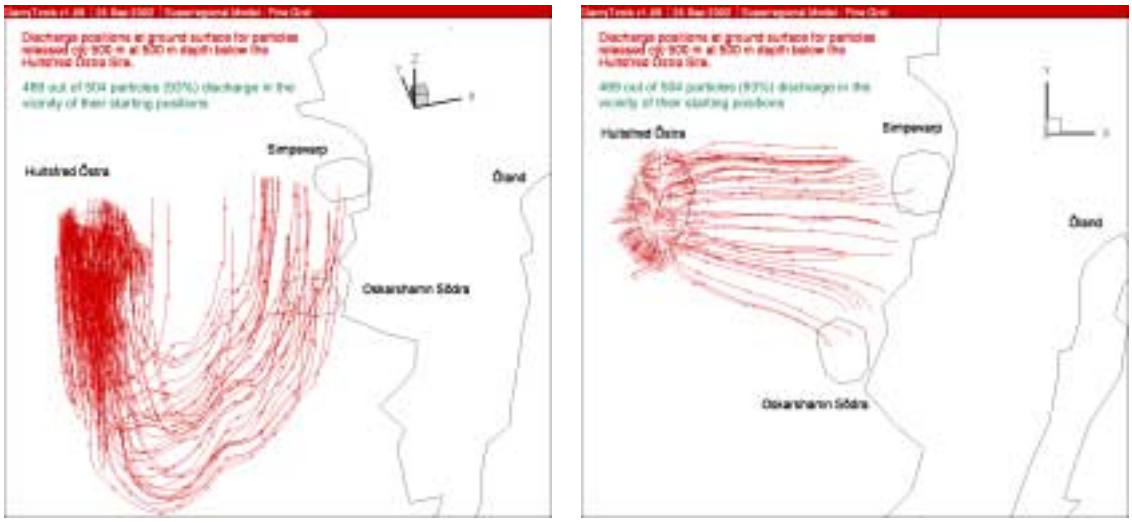

Figure 4-14. *Perspective view and plane view of the particle pathways and their discharge locations using Model B at a time slice of 40 ka.*

4.5 On the role of using variable-density models

In order to take account for the buoyancy forces it is necessary to include a variable-density formulation in the governing equations. Figure 4-15 shows a comparison between particle pathways for two runs with Model B – one without salinity and the other with.

The freshwater case shown in Figure 4-15 renders that as much as c 70% of the particles discharge in the immediate vicinity of their starting positions. This suggests that a correct representation of the local variations in the topography is very important for finding *realistic discharge locations*. On the other hand, the salinity case shown in Figure 4-15 renders that *realistic pathway properties, fluxes and advective travel times* between the source and the sink can only be expected if variable-density is taken into account.

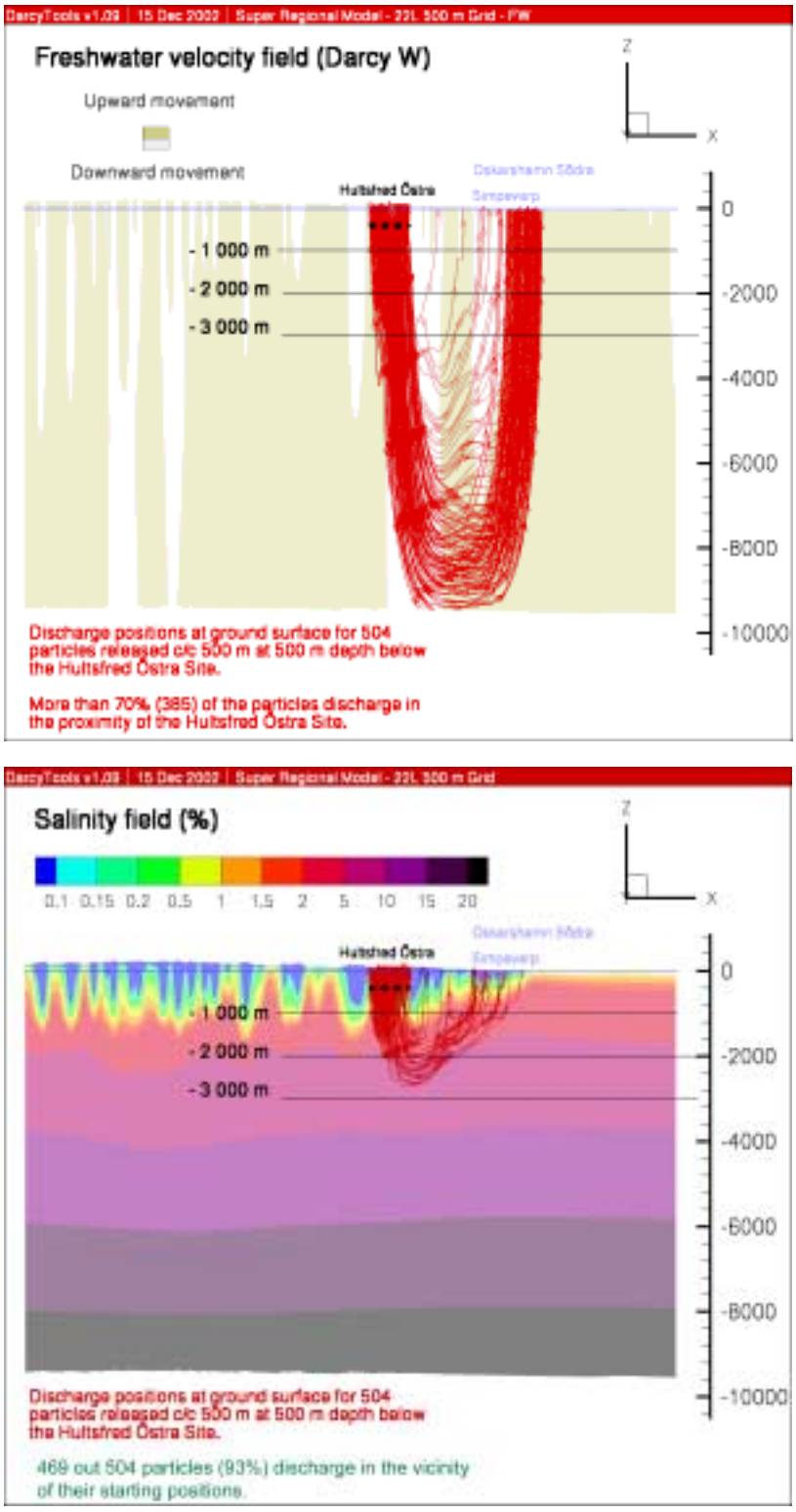

Figure 4-15. *Comparison between particle pathways for two runs with Model B – one without salinity (top) and the other with (bottom). Realistic pathway properties, fluxes and advective travel times can only be expected if variable-density is taken into account.*

5 Discussion and conclusions

Comparative simulations were run for two mesh discretisations, thus honouring the local-scale variations in the topography differently. The model with the coarser mesh discretisation was used to mimic the model of /Voss and Provost, 2001/. The model with the finer mesh discretisation was used to scrutinise the former. In addition, the role of variable-density flow was studied by running some of the simulations without salinity. The role of the mesh discretisation is known to be important in numerical modelling. Voss and Provost used a finer discretisation in the vicinity of the exploratory sites and in the network of stream valleys that runs among the sites, which was expected to strongly affect the flow field. Voss and Provost commented that the mesh used, still must be considered a rather coarse discretisation of the region and the results should not be seen as uniformly accurate. Notwithstanding, in the discussion of the results, they advocated that their simulations are strongly indicative. In a way the present study can be regarded as a follow-up study to Voss and Provost's wish to use a much finer mesh with more regular areal discretisation in order to improve the correctness.

An analysis of the topography along a profile running from west to east across the model area shows that local topographic gradients of Östra Götaland are strongly indicative of local flow cells and that the result of numerical modelling is likely to be dependent on the chosen resolution of the mesh discretisation. On top of this lies the hydrogeological fact that the fabric is not porous but consists of fracture crystalline rock, which is highly anisotropic. An important factor associated with the occurrence of vertical fractures zones, however, is that the majority of these occur in valleys, hence strengthening the pattern of local flow cells. This important fact is overlooked by Voss and Provost, who treated anisotropy as a uniformly distributed entity, which is not consistent with field data.

The reader is referred to /p 27 of Voss and Provost, 2001/ for a detailed description of the motive for the no-flow boundary condition as well as the "salt generator" used. From a hydrogeological point of view, we would like to bring the reader's attention to two issues, the effects of which are not clear from the report. First, the no-flow boundaries in the southwest effectively reroutes the natural regional runoff towards the eastern shoreline, thus causing an unrealistic regional flow pattern in this part of the model domain. This approximation may be advocated to be insignificant for the flow below the four exploratory sites, which are located more or less in the centre of the model domain. However, such a rationale is not tested by Voss and Provost by means of a sensitivity study, which is a pity with regards to the precise conclusions drawn.

Second, the 'salt generator' used by Voss and Provost suppresses mixing by advection as the main mechanism for explaining the groundwater chemistry, an assumption that is not obvious given resent research results. Moreover, the mass transfer coefficient k, which is a rate constant for the production of salt, has a very long time scale. The value of k for the isotropic case mimicked here renders that c 6–7 Ma are required in order to alter the salinity by 1% at depth assuming no advection. Closer to land surface c 1–1.5 Ma are needed. The implication of the 'salt generator' is that the simulation time needed to reach a steady-state flow and solute concentration becomes extremely sensitive to the initial condition of salinity.

Voss and Provost stated that they simulated a steady-state flow and solute concentration to represent present-day conditions, and that the repository siting was then evaluated on the basis of this flow field. The amount of time elapsed in the present interglacial, i.e. c 14 ka, may be sufficient to reach a steady state. However, given the strong impact of the ongoing rebound process, a word of caution about the present-day conditions being at a steady state seems logical. The shoreline displacement process is expected to alter the topography of Östra Götaland by c 15 m during the next 10 ka.

Particle tracking results are presented in the present study for two of the four exploratory sites studied by Voss and Provost, namely the Comparison site and Hultsfred Östra. Particle tracking results for Oskarshamn Södra and Simpevarp are not treated in detail, but an approximate study is found in Appendix A, which presents a comparison between the computer code used to study the regional-scale groundwater flow pattern in Northern Uppland and the computer code used in the present study. The results shown in Appendix A reveal that the two codes give identical results for the problem studied, implying that many results obtained from the detailed study of Northern Uppland probably are of generic importance.

In our opinion, the results presented in this study indicate that the conclusions drawn by Voss and Provost appear to suffer from not only an insufficient mesh discretisation but possibly also from an insufficient simulation time. This conclusion is particularly true for the Comparison site, which suffers more from an irregular mesh discretisation, strong transients in the variable-density field and uncertain boundary conditions than Hultsfred Östra.

The simulations presented in this study using a refined mesh discretisation yield that the vast majority of the particles released at repository depth below the two sites discharge at land surface in the vicinity of their starting positions. The conclusion drawn here is that local flow cells appear to occur throughout Östra Götaland, even at pronounced high altitude inland locations, which implies that it is the hydrogeological properties at each site that will by and large determine the transport times. In order to get all of the important pathway properties correctly modelled (the travel times, the Darcy fluxes at the repository level and the F-factors of the pathways), it is our opinion that it is necessary to account for variable-density flow in the mass and salt conservation equations.

Finally, the model applications used by Voss and Provost as well as the one used here constitute continuum approximations. This means that the extremely discrete and anisotropic behaviour, which characterises groundwater flow through sparsely fractured crystalline rock on a detailed scale, is not accounted for. Consequently, the conclusions of this study concern above all physical phenomena of principal interest. On the scale treated, we consider the continuum approach applicable.

6 References

Follin S, Svensson U, 2002. Groundwater flow simulations in support of the Local Scale Hydrological Description developed within the Laxemar Methodology Test Project, SKB R-02-29, Svensk Kärnbränslehantering AB.

Freeze R A, Witherspoon P A, 1967. Theoretical Analysis of Regional Groundwater Flow. 2. Effect of Water-Table Configuration and Subsurface Permeability Variation. Water Resources Research, Vol 3, No 2. pp 623–634.

Gustafsson Y, 1970. Topografins inverkan på grundvattenbildningen. Grundvatten, P A Norstedt & Söners förlag. Stockholm.

Holmén J G, 1997. On the flow of groundwater in closed tunnels. Generic hydrogeological modelling of nuclear waste repository, SFL 3-5, SKB TR-97-10, Svensk Kärnbränslehantering AB.

Holmén J, Stigsson M, Gylling B, Marsic N, 2003. Modelling of groundwater flow and flow paths for a large regional domain in Northeast Uppland, SKB R-03-24, Svensk Kärnbränslehantering AB.

Laaksoharju M, 1999. Groundwater characterisation and modelling: problems, facts and possibilities, SKB TR-99-42, Svensk Kärnbränslehantering AB.

LMV, 2000. GSD-Elevation database. Lantmäteriet, SE 801 82 Gävle, Sweden.

Provost A M, Voss C I, Neuzil C E, 1998. Glaciation and regional ground-water flow in the Fennoscandian shield. SKI Report 96:11, Swedish Nuclear Power Inspectorate, Stockholm.

Påsse T, 1996. A mathematical model of the shore level displacement in Fennoscandia, SKB TR-96-24, Svensk Kärnbränslehantering AB.

Rehbinder G, Follin S, Isaksson A, 1997. On regional flow in Baltic Shield rock. An application of an analytical solution using hydrogeologic conditions at Aberg, Beberg and Ceberg of SR 97, SKB R-97-17, Svensk Kärnbränslehantering AB.

Rhén I, Gustafson G, Stanfors R, Wikberg P, 1997. Äspö HRL – Geoscientific evaluation 1997/5. Models based on the site characterisation 1986–1995, SKB TR-97-06, Svensk Kärnbränslehantering AB.

SKB, 2000. Samlad redovisning av metod, platsval, och program inför platsundersökningsskedet. Svensk Kärnbränslehantering AB.

Svensson U, Kuylenstierna H-O, Ferry M, 2002. DarcyTools, Concepts, methods, equations and tests. Version 1.0. Draft report submitted to SKB March 2002, Svensk Kärnbränslehantering AB.

Tóth J, 1963. A theoretical analysis of groundwater flow in small drainage basins. Journal of Geophysical Research 68, pp 4795–4812.

Tóth J, Sheng G, 1994. Enhancing nuclear waste disposal safety by exploiting regional groundwater flow – An exploratory proposition. Annual Int Conf, Fifth, High-level Radioactive Waste Management, Proc, Las Vegas, Nevada, 1994: American Nuclear Society, Inc and American Society of Civil Engineers, pp 1797–1804.

Tóth J, Sheng G, 1996. Enhancing safety of nuclear waste disposal by exploiting regional groundwater flow: The Recharge Area Concept. Hydrogeology J. Vol 4, No 4.

Voss C I, Andersson J, 1993. Regional Flow in the Baltic Shield During Holocene Coastal Regression. Ground Water, Vol 31, No 6.

Voss C I, Provost A M, 2001. Recharge-area nuclear waste repository in Southeastern Sweden, Demonstration of hydrogeologic siting concepts and techniques, SKI Report 01:44, Swedish Nuclear Power Inspectorate, Stockholm.

Voss, 2002. Personal communications.

Zijl W, 1999. Scale aspects of groundwater flow and transport systems. Hydrogeology Journal 7:139–150, Springer-Verlag.

Appendix A

Comparative numerical simulations

Background

A comparison was made in order to cross-validate the numerical codes Geoan /Holmén, 1997/ and DarcyTools /Svensson et al, 2002/ used for regional-scale groundwater flow studies of Northern Uppland and Östra Götaland, respectively, and thereby also corroborate the simulation results from the two studies in a numerical perspective. The results of the regional-scale groundwater flow study of Northern Uppland are reported in /Holmén et al, 2003/.

Model setup

The chosen model domain for the comparison is shown in Figure A-1. The thick red line in Figure A-1 represents the regional drainage area for Simpevarp. Hultsfred Östra and Oskarshamn Södra are situated on the border of the main drainage area.

The numerical resolution of the flow models was set to 330 m. The topographic variations on the top surface were based on the 50 m Digital Terrain Model /LMV, 2000/. The groundwater flow simulations were made with a simplified flow model assuming freshwater flow at a steady state through a homogeneous and isotropic medium. The elevation of the bottom surface was set to –1 100 m a s l.

The boundary conditions for the DarcyTools simulations were prescribed head on the top surface and on all vertical surfaces and no flow on the bottom surface. The DarcyTools flow model consisted of 22 layers with thicknesses ranging from 15–100 m. The boundary conditions for the Geoan simulations were prescribed head on the top surface and on the vertical surface facing the Baltic Sea and no flow on the bottom surface and the remaining vertical surfaces below the perimeter of the regional drainage area. The Geoan flow model consisted of 11 layers with thicknesses ranging between 50–240 m.

Visualisation of results

The distribution of recharge and discharge within the model domain are shown for two levels below the top surface; 7.5 m and 515 m, see Figures A-1 and Figure A-2. Grey represents recharging conditions and olive green discharging. The colouring was determined by the sign of the vertical component of the Darcy velocity vector.

Discharge locations for particles released c/c 330 m at c 500 m depth below the top surface are shown in Figure A-3 and Figure A-4. The simulations were made with DarcyTools and Geoan, respectively.

Finally, discharge locations and statistics for 172 particles released c/c 330 m at 515 m depth below the top surface along a profile between Hultsfred Östra and Simpevarp are shown in Figure A-5. 48% of the particles go downwards before they go up again. 11% pass the bottom layer before they exit at the top surface.

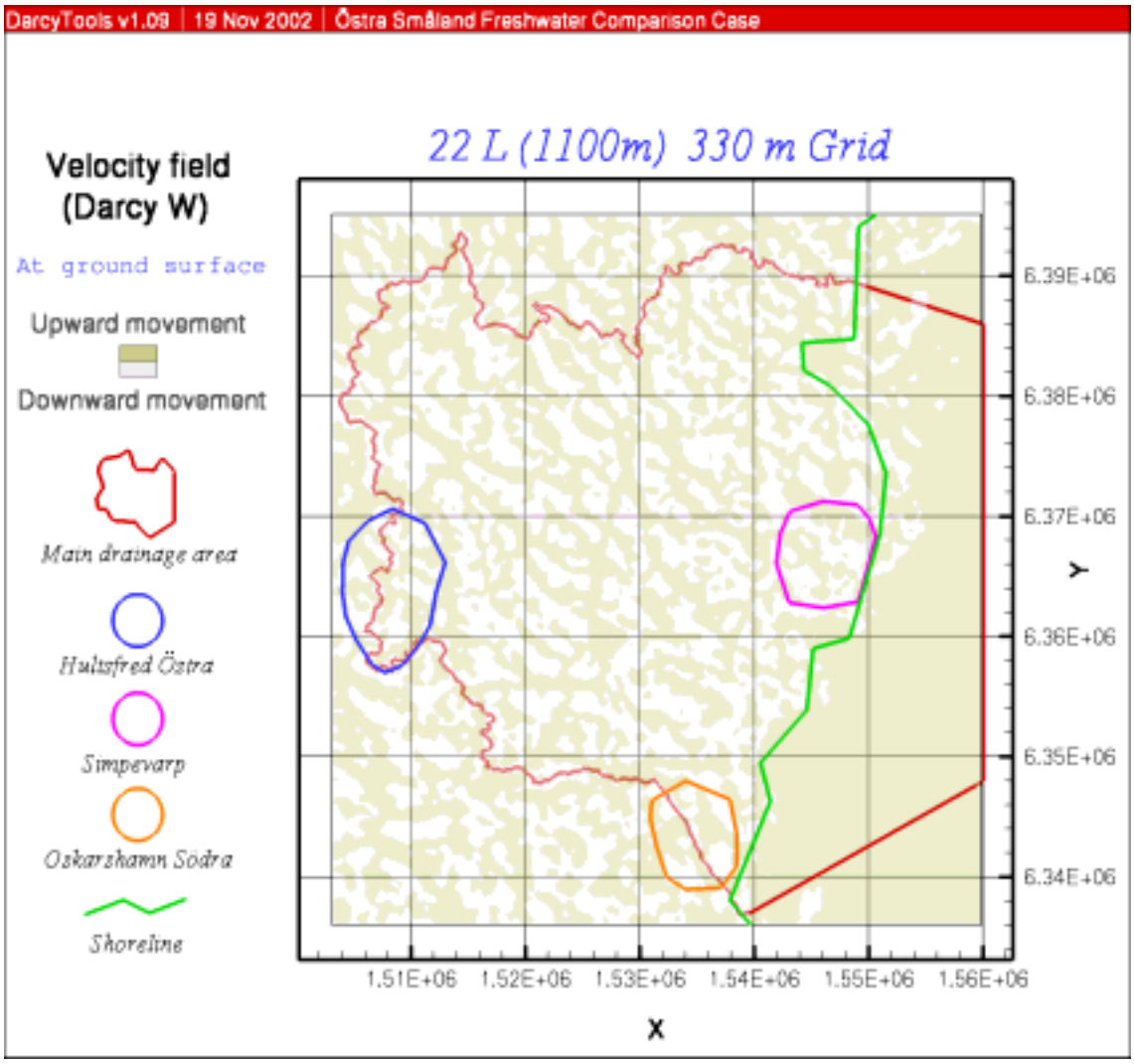

Figure A-1. *The distribution of recharge and discharge within the model domain at 7.5 m below the top surface using DarcyTools. Grey represents recharging conditions and olive green discharging. The colouring was determined by the sign of the vertical component of the Darcy velocity vector.*

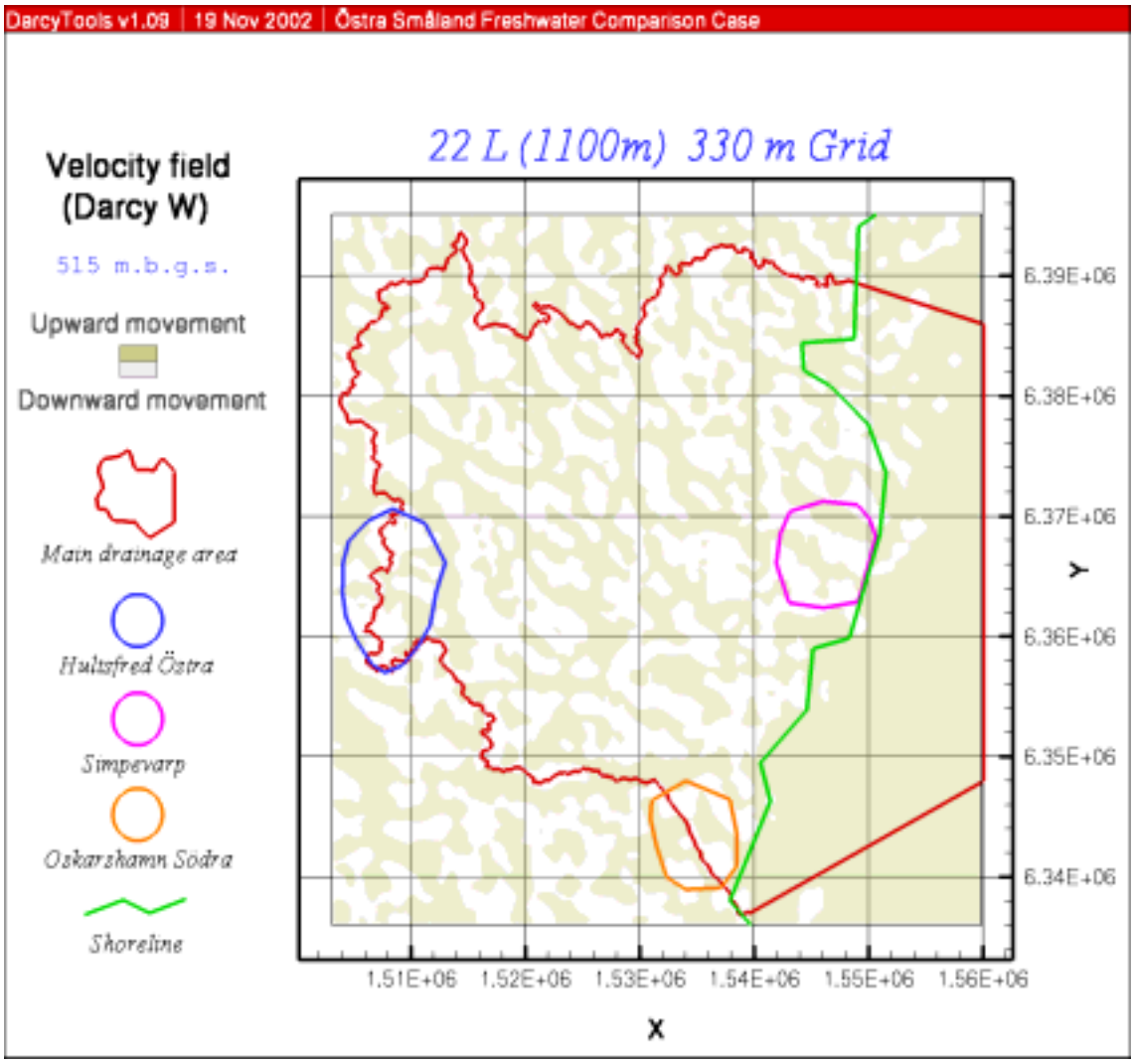

Figure A-2. *The distribution of recharge and discharge within the model domain at 515 m depth below the top surface using DarcyTools. Grey represents recharging conditions and olive green discharging. The colouring was determined by the sign of the vertical component of the Darcy velocity vector.*

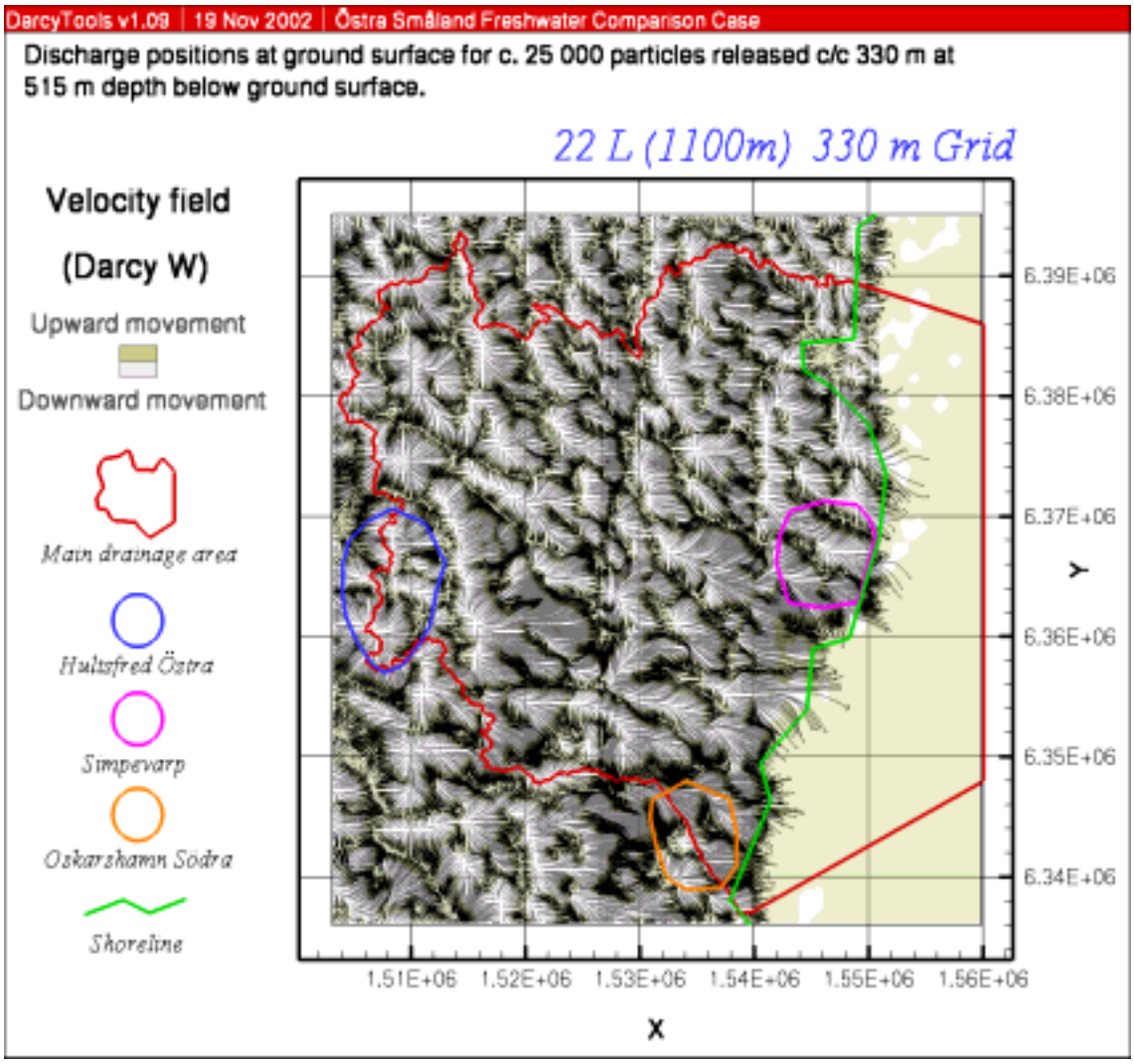

Figure A-3. *Discharge locations for c 25 000 particles released c/c 330 m at 515 m depth below the top surface. The simulation was made with* ***DarcyTools*** *and the visualisation of the pathways was made with Tecplot.*

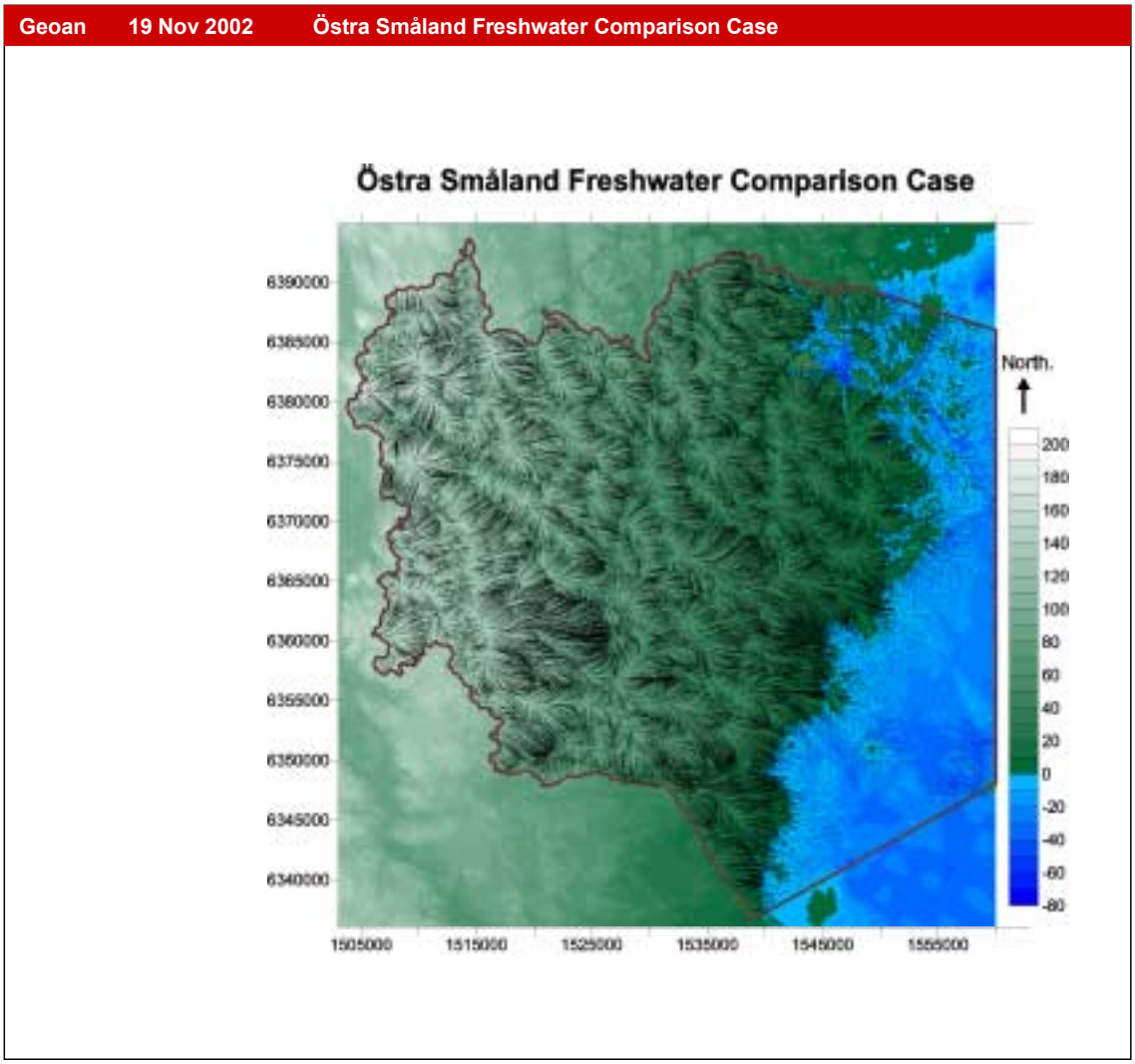

Figure A-4. *Discharge locations for c 15 500 particles randomly released between 490–540 m depth below the top surface. The simulation was made with* ***Geoan*** *and the visualisation was made with Surfer.*

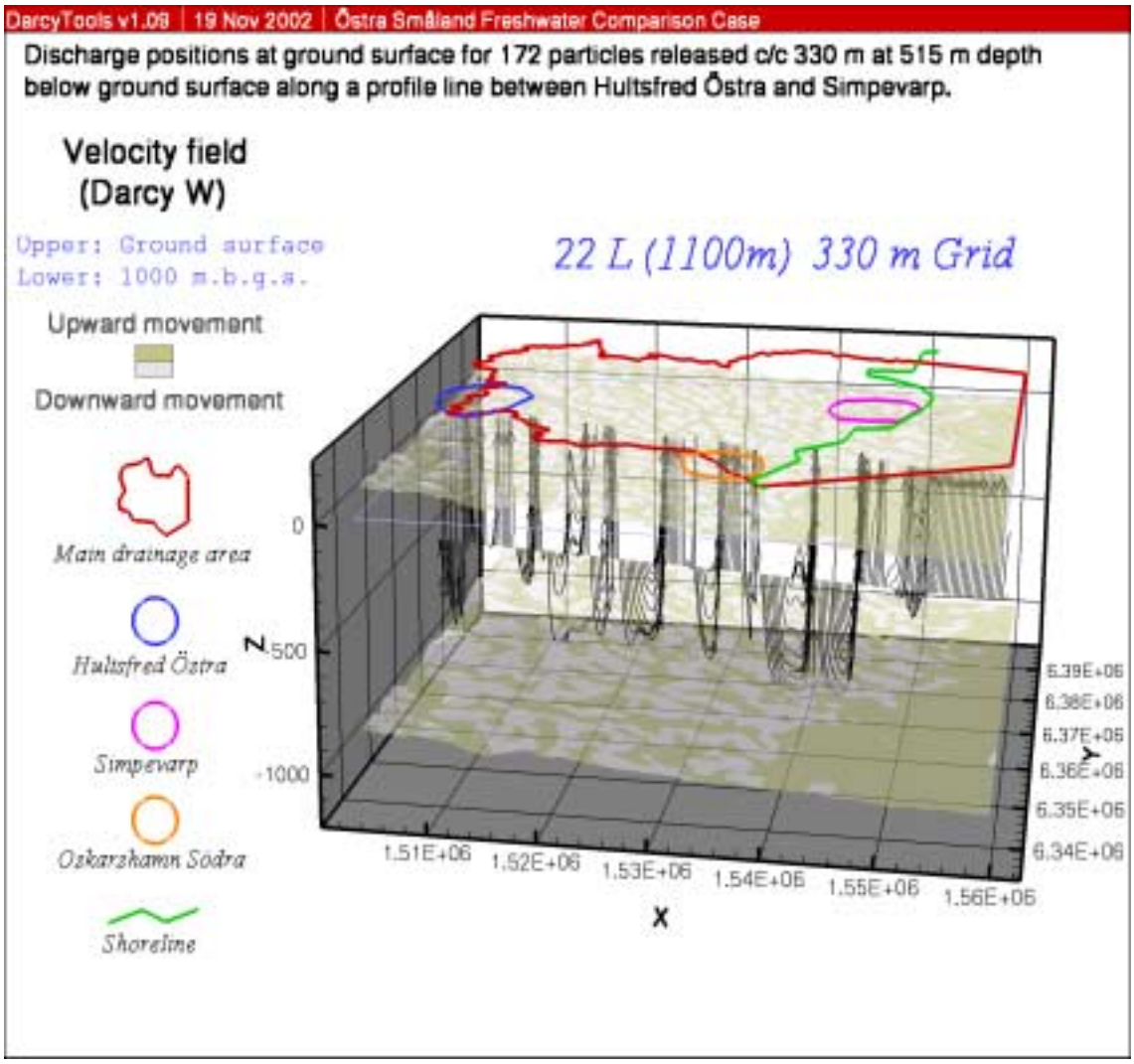

Figure A-5. *Discharge locations for 172 particles released c/c 330 m at 515 m depth below the top surface along a profile between Hultsfred Östra and Simpevarp using DarcyTools.*

Appendix B

Recharge and discharge within the regional drainage area of Simpevarp

Background

High-resolution numerical simulations of the recharge and discharge conditions in the vicinity of the Simpevarp candidate area were conducted on behalf of SKB in January 2003 as a result of an oral presentation to the Swedish authorities in December 2002. It is noted that the work presented in this appendix is an extension of the original scope of the present study, which was not intended to deal with the site selection process as such.

Model setup

The model domain shown in Figure B-1 exceeds the main drainage area of the Simpevarp candidate area. The thick black line represents the main drainage area and the thin red line is the Simpevarp candidate area.

The numerical resolution of the flow model was 100 m. The topographic variations shown in Figure B-1 were based on the 50 m Digital Terrain Model by /LMV, 2000/. The groundwater flow simulations were made with a simplified flow model assuming freshwater flow at a steady state through a homogeneous and isotropic medium. The boundary conditions were as follows: prescribed head on the top surface and on the vertical surfaces and no flow on the bottom surface. The flow model consisted of 22 layers with thicknesses ranging from 15–100 m. The elevation of the bottom surface was set to –1 100 m a s l.

Visualisation of results

The distribution of recharge and discharge within the model domain are shown for three levels below the top surface; 15 m, 500 m and 950 m, see Figures B-2 through Figure B-4. Grey represents recharging conditions and olive green discharging. The colouring was determined by the sign of the vertical component of the Darcy velocity vector.

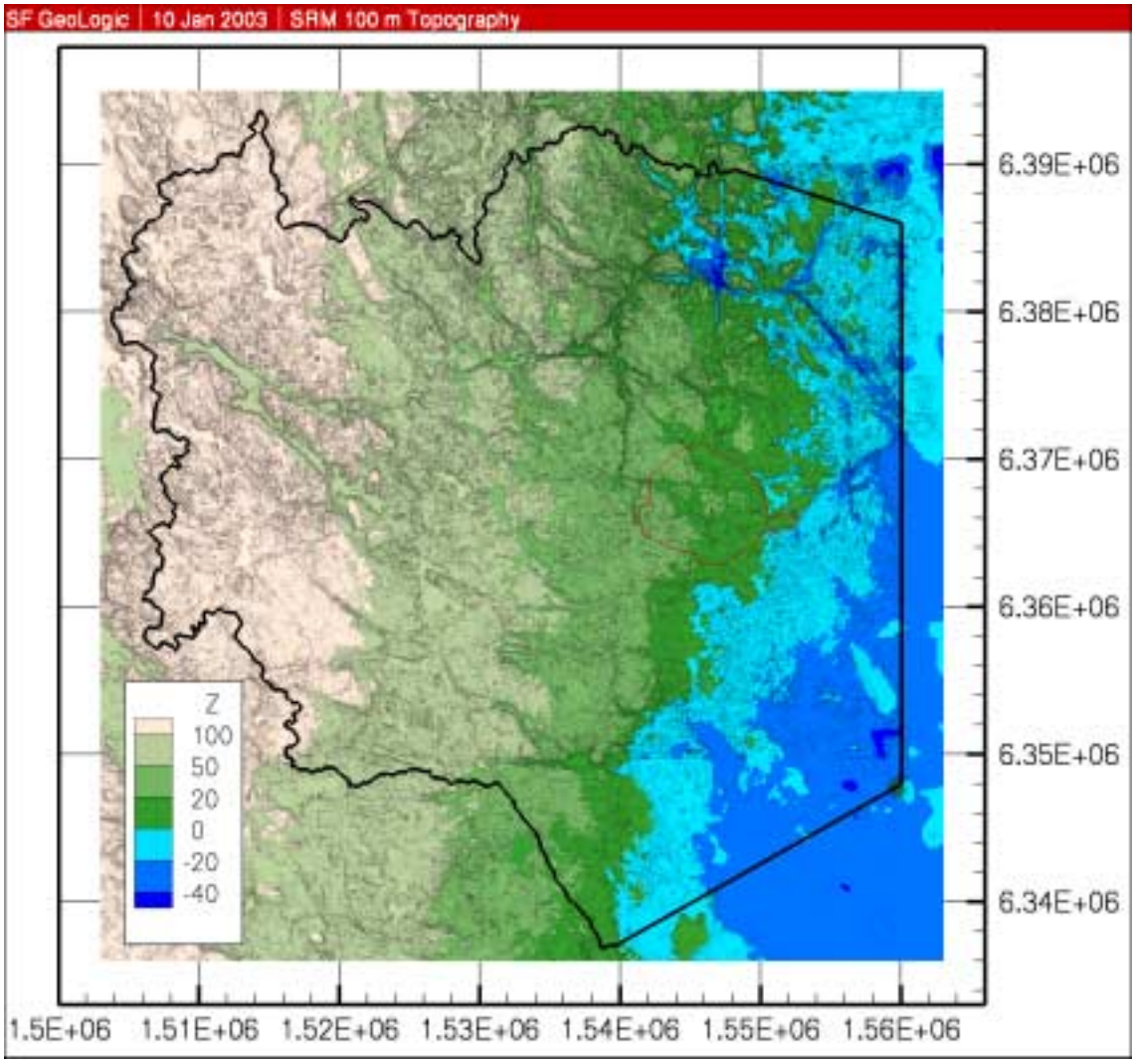

Figure B-1. *The model domain exceeds the main drainage area of the Simpevarp candidate area. The thick black line represents the main drainage area and the thin red line is the Simpevarp candidate area. The numerical resolution of the flow model was 100 m.*

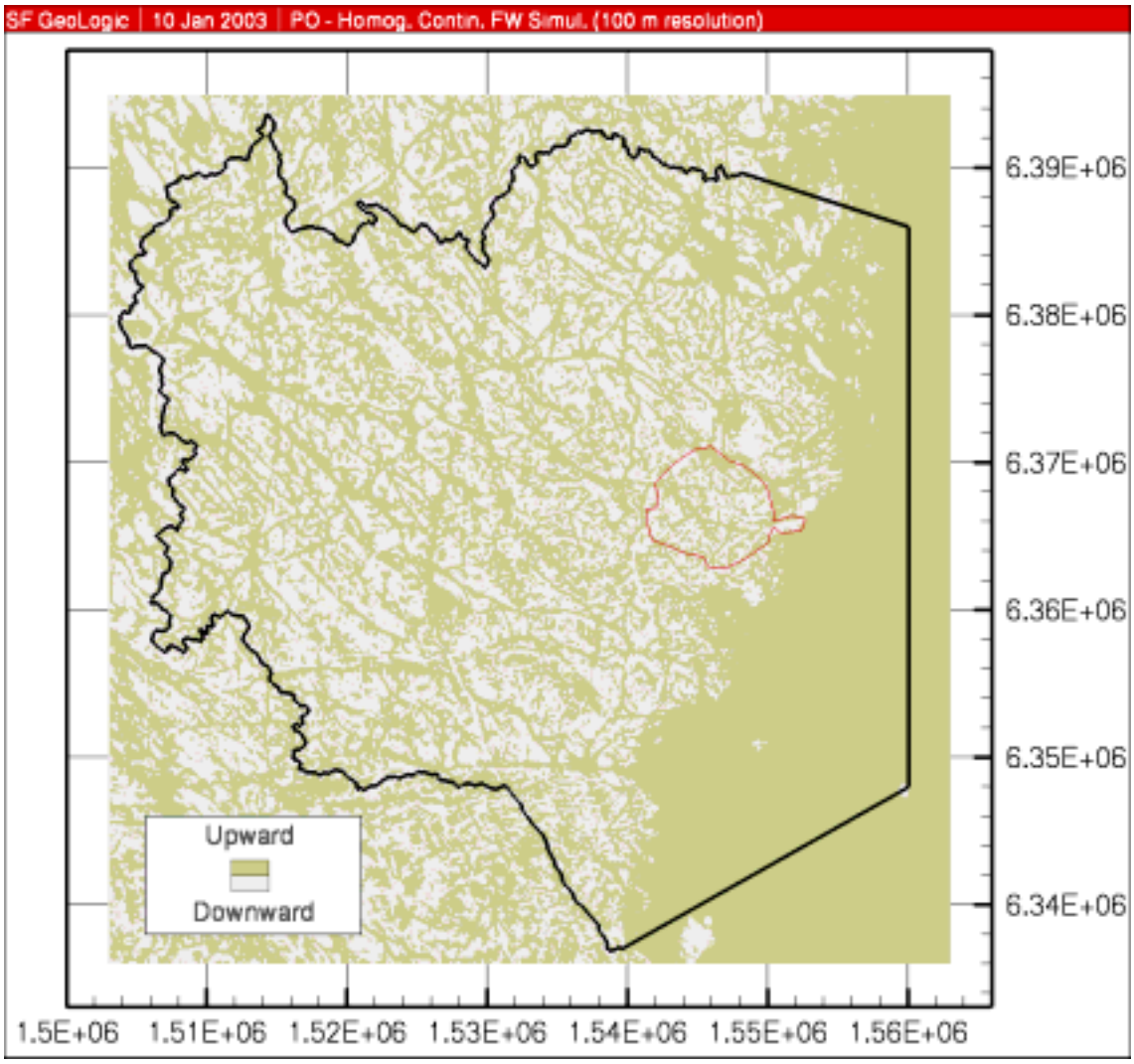

Figure B-2. *The distribution of recharge and discharge areas within the model domain at 15 m depth below the top surface. Grey represents recharging conditions and olive green discharging. The colouring was determined by the sign of the vertical component of the Darcy velocity vector.*

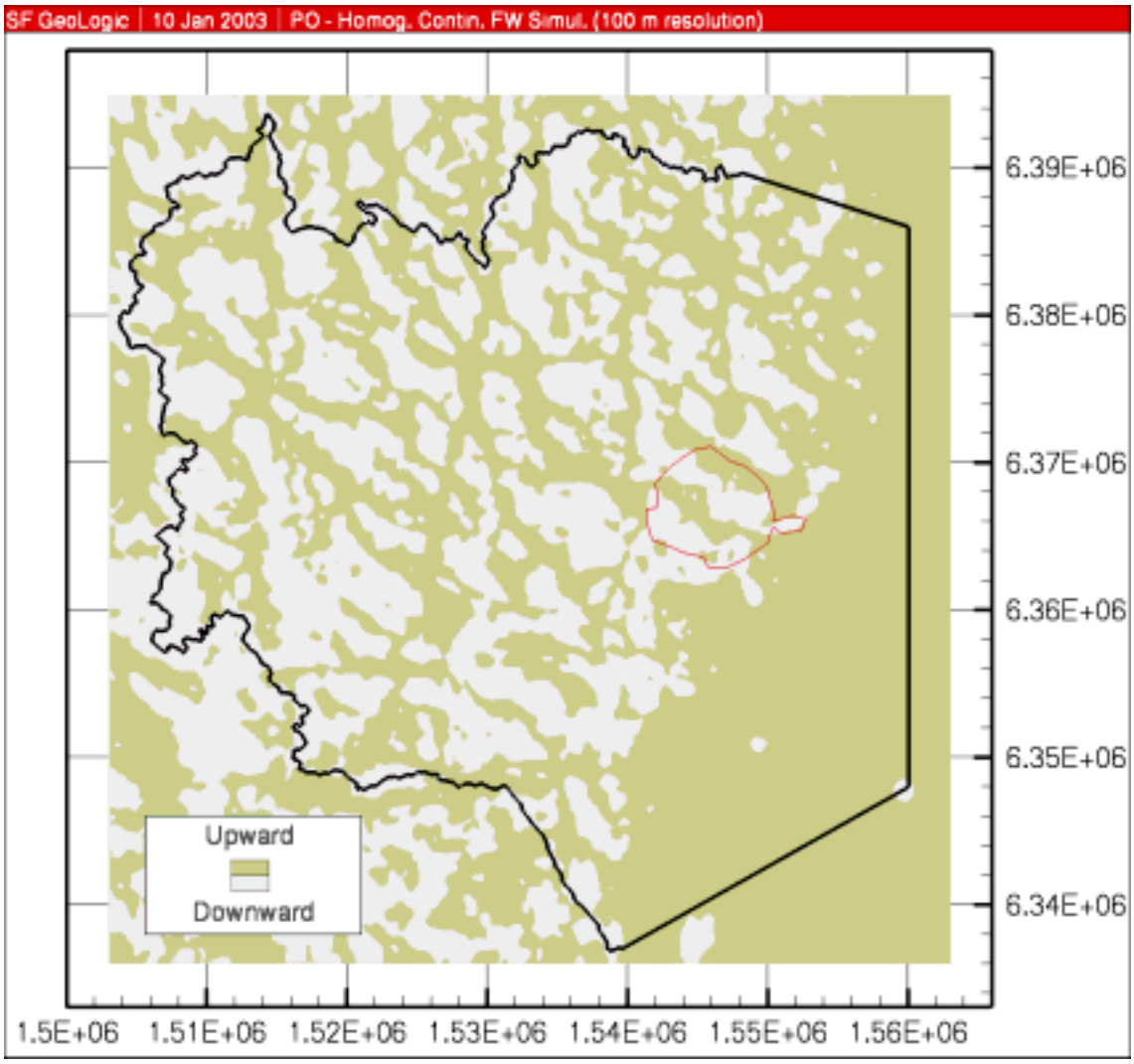

Figure B-3. *The distribution of recharge and discharge within the model domain at 500 m depth below the top surface. Grey represents recharging conditions and olive green discharging. The colouring was determined by the sign of the vertical component of the Darcy velocity vector.*

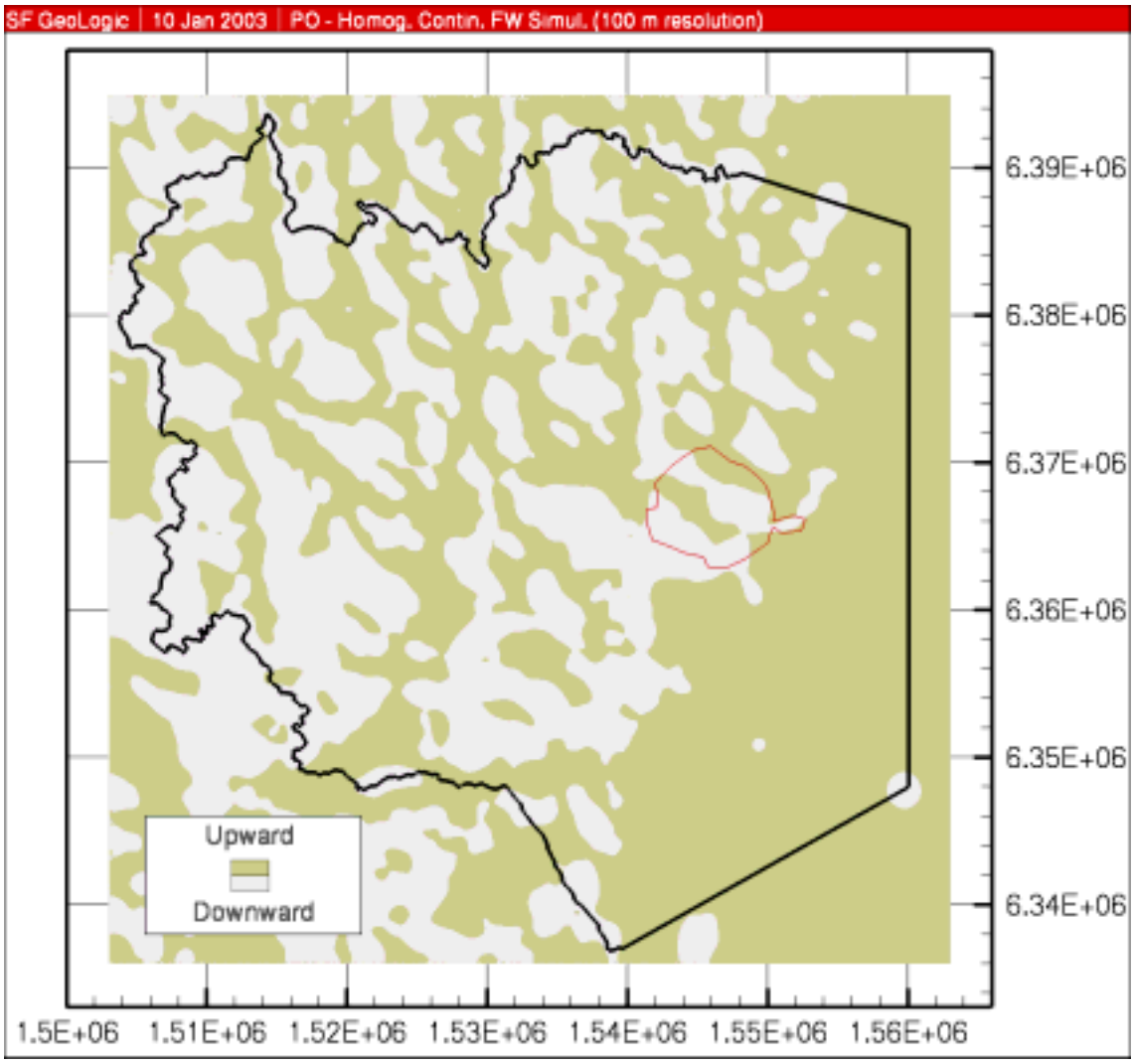

Figure B-4. *The distribution of recharge and discharge within the model domain at 900 m depth below the top surface. Grey represents recharging conditions and olive green discharging. The colouring was determined by the sign of the vertical component of the Darcy velocity vector.*